Root-associated fungal microbiota of nonmycorrhizal *Arabis alpina* and its contribution to plant phosphorus nutrition

Juliana Almario[a,b,1], Ganga Jeena[a,b], Jörg Wunder[c], Gregor Langen[a,b], Alga Zuccaro[a,b], George Coupland[b,c], and Marcel Bucher[a,b,2]

[a]Botanical Institute, Cologne Biocenter, University of Cologne, 50674 Cologne, Germany; [b]Cluster of Excellence on Plant Sciences, University of Cologne, 50674 Cologne, Germany; and [c]Department of Plant Developmental Biology, Max Planck Institute for Plant Breeding Research, 50829 Cologne, Germany

Edited by Luis Herrera-Estrella, Center for Research and Advanced Studies, Irapuato, Guanajuato, Mexico, and approved September 1, 2017 (received for review June 9, 2017)

Most land plants live in association with arbuscular mycorrhizal (AM) fungi and rely on this symbiosis to scavenge phosphorus (P) from soil. The ability to establish this partnership has been lost in some plant lineages like the Brassicaceae, which raises the question of what alternative nutrition strategies such plants have to grow in P-impoverished soils. To understand the contribution of plant–microbiota interactions, we studied the root-associated fungal microbiome of *Arabis alpina* (Brassicaceae) with the hypothesis that some of its components can promote plant P acquisition. Using amplicon sequencing of the fungal internal transcribed spacer 2, we studied the root and rhizosphere fungal communities of *A. alpina* growing under natural and controlled conditions including low-P soils and identified a set of 15 fungal taxa consistently detected in its roots. This cohort included a Helotiales taxon exhibiting high abundance in roots of wild *A. alpina* growing in an extremely P-limited soil. Consequently, we isolated and subsequently reintroduced a specimen from this taxon into its native P-poor soil in which it improved plant growth and P uptake. The fungus exhibited mycorrhiza-like traits including colonization of the root endosphere and P transfer to the plant. Genome analysis revealed a link between its endophytic lifestyle and the expansion of its repertoire of carbohydrate-active enzymes. We report the discovery of a plant–fungus interaction facilitating the growth of a nonmycorrhizal plant under native P-limited conditions, thus uncovering a previously underestimated role of root fungal microbiota in P cycling.

Brassicaceae | microbiome | fungal endophyte | Helotiales | nutrient transfer

Comparable with the human microbiota, millions of microbes colonize plants and form complex communities on plant surfaces and in plant tissues. The interactions between the plant and its microbiota range from parasitism (detrimental to the host) to mutualism (mutually beneficial), and their outcome can be pivotal for plant performance. Plant-associated microbes can influence plant fitness by modulating plant growth, root architecture, nutrient acquisition, or drought and disease resistance (1–3). Thus, the plant microbiota can be seen as an extension of the plant genome in the sense that it can increase the plant's adaptation capacity (4). This is illustrated by the arbuscular mycorrhizal (AM) symbiosis established between land plants and Glomeromycota fungi, which is thought to have facilitated the adaptation of plants to a terrestrial life (5). It is estimated that 80% of the vascular plant species (6) receive phosphorus (P) and other nutritional elements from these fungi in exchange for photosynthates (7). The ability to form an AM symbiosis has been lost independently in several flowering plant lineages including the Brassicaceae family through the loss of essential symbiosis genes during evolution (8). Given the beneficial effect of AM fungi on plant P uptake, the question of whether nonmycorrhizal species thrive due to the exploitation of alternative P-mining strategies forms the basis of current research (9). In the context of the plant holobiont, i.e., the plant and all its microbial partners, models of plant nutrition need to account for these cross-kingdom interactions to be complete. Here, we integrate these concepts and study the role of root-associated fungi other than AM in plant P nutrition.

In some plant lineages, AM co-occurs with other mycorrhizal symbioses like ectomycorrhiza (woody plants), orchid mycorrhiza (orchids), and ericoid mycorrhiza (Ericaceae) (10). These associations can also promote plant nutrition; however, they have not been described in Brassicaceae. Endophytic microbes can promote plant P acquisition by different processes including P solubilization and mineralization (11) or transfer of P in the form of soluble orthophosphate. P transfer to their hosts was considered a hallmark of mycorrhizal fungi until recently. Two studies on binary root–fungus interactions showed that two endophytes—the Ascomycete *Colletotrichum tofieldiae* (12) and the Basidiomycete *Serendipita indica* (syn. *Piriformospora indica*) (13)—are able to transfer P to their nonmycorrhizal host *Arabidopsis thaliana*, promoting its growth under low-P conditions. *S. indica* was also demonstrated to participate in P uptake of maize plants depending on the expression of a fungal high-affinity phosphate transporter (14). These studies provided proof of concept for P transfer from fungi to nonmycorrhizal hosts; however, the ecological relevance of these interactions remains unclear as it is not known whether these endophytes can promote plant P uptake under native low-P soil conditions, and only *C. tofieldiae* was shown to be a natural inhabitant of *A. thaliana* roots. Descriptive and functional studies

Significance

Most terrestrial plants live in symbiosis with arbuscular mycorrhizal (AM) fungi and rely on this association to scavenge the macronutrient phosphorus (P) from soil. *Arabis alpina* thrives in P-limited alpine habitats, although, like all Brassicaceae species, it lacks the ability to establish an AM symbiosis. By studying the fungal microbiota associated with *A. alpina* roots we uncovered its association with a beneficial Helotiales fungus capable of promoting plant growth and P uptake, thereby facilitating plant adaptation to low-P environments.

Author contributions: J.A., A.Z., G.C., and M.B. designed research; J.A., G.J., and J.W. performed research; J.A. and G.J. contributed new reagents/analytic tools; J.A., G.J., and G.L. analyzed data; and J.A. and M.B. wrote the paper.

The authors declare no conflict of interest.

This article is a PNAS Direct Submission.

Freely available online through the PNAS open access option.

Data deposition: The sequence reported in this paper has been deposited in the National Center for Biotechnology Information under Bioproject PRJNA386947 and PRJNA378526.

See Commentary on page 11574.

[1]Present address: Department of Plant Microbe Interactions, Max Planck Institute for Plant Breeding Research, 50829 Cologne, Germany.

[2]To whom correspondence should be addressed. Email: m.bucher@uni-koeln.de.

This article contains supporting information online at www.pnas.org/lookup/suppl/doi:10.1073/pnas.1710455114/-/DCSupplemental.

on the fungal microbiota of nonmycorrhizal plants are needed to improve our understanding of the ecological relevance of these interactions for plant nutrition at the holobiont level.

Although fungi represent a prominent part of the root microbiota where they can play important roles as pathogenic or beneficial partners, studies of Brassicaceae species have focused mainly on bacterial communities (1, 15–17). These studies have increased our knowledge of how root bacterial communities are shaped by environmental, edaphic, and host-related factors. Expansion of this knowledge to fungal communities is crucial as studies on the mycorrhizal host species poplar (18), sugar cane (19), and *Agave* (20) suggest that fungal and bacterial root communities respond differently to environmental cues. Microbiome studies focusing on taxonomical description have shown that fungi detected in plant tissues are often phylogenetically related to described plant pathogens or saprotrophs (3, 18). Comparative genomics analyses have shown that plant beneficial endophytic lifestyles can emerge from plant pathogenic or saprophytic fungal lineages through genome modifications often involving the expansion or contraction of gene families encoding carbohydrate active enzymes (CAZymes) involved in plant cell-wall degradation (21–23). Prediction of the ecological role of fungal root endophytes is thus challenging and requires more systematic studies associating endophyte isolation, in planta testing, and genomic investigation.

Arabis alpina (Brassicaceae) is a nonmycorrhizal perennial arctic-alpine herb growing in harsh and rocky environments (24) including P-impoverished soils (this study). In recent years it has emerged as a model for ecological and developmental studies, and its genome has recently been sequenced (25). The aim of the present study was to explore the root fungal microbiome of *A. alpina* and its contribution to plant P acquisition, following the hypothesis that root-associated fungi other than AM fungi can promote plant P uptake under natural and controlled low-P conditions. We used Illumina-based amplicon sequencing of the fungal taxonomical marker internal transcribed spacer 2 (ITS2) to describe the fungal microbiome in *A. alpina* roots (endosphere) and the rhizosphere (soil zone immediately surrounding the root) under greenhouse, common garden, and natural conditions. Microbiome variability analysis showed that root fungal communities were more robust in response to changing environments relative to the rhizosphere assemblages, leading to the description of a set of 15 fungal taxa consistently detected in *A. alpina* roots. Within this cohort we identified a fungal taxon belonging to the Helotiales order, exhibiting high abundance in the roots of wild *A. alpina* plants growing in an extremely P-limited soil. Successful isolation of a specimen from this taxon from *A. alpina* roots, followed by its reintroduction into the native P-limited soil after sterilization, promoted *A. alpina* growth and shoot P accumulation. In vitro studies further demonstrated that the fungus' contribution to plant growth involves transfer of inorganic phosphate to its host. Finally, fungal genome sequencing revealed an expansion of its repertoire of carbohydrate-active enzymes, which may be associated with its endophytic lifestyle. Cumulatively, these results provide evidence for a beneficial role of a hitherto unknown member of the root microbiota in *A. alpina* growth performance in low-P environments.

Results

Root-Associated Fungal Communities in *A. alpina* Were Unaffected by Host Genetic Variation. Our current understanding of the structure of the root microbiome in nonmycorrhizal Brassicaceae species rests primarily on bacterial communities, and information on the factors shaping root-associated fungal consortia is scarce. We studied fungal communities associated with *A. alpina* roots by sequencing the fungal ITS2 with primers ITS9/ITS4 as they showed a better recovery of low-abundance fungal diversity in comparison with other primers in a pilot experiment (*SI Appendix*, Fig. S1).

We assessed the effect of plant intraspecific variation on the structure of the root-associated fungal community by comparing four European *A. alpina* accessions (Fig. 1*A* and *SI Appendix*, Table S1) grown side by side at the Lautaret common garden (GAR-Lau). At harvest time, the accessions differed in size and developmental stage (*SI Appendix*, Fig. S2*D*) but shared similar root and rhizosphere fungal communities with comparable diversity (ANOVA $P > 0.05$) (*SI Appendix*, Fig. S2*B*) and structure, as observed in the principal coordinates analysis (PCoA) (*SI Appendix*, Fig. S2*A*) and verified by permutational multivariate analysis of variance (PERMANOVA) results ($P > 0.05$). This indicated that, under the assessed seminatural common garden conditions, host genetic variation fails to impact the root-associated fungal community in *A. alpina*. This contrasted with studies in which a small but significant contribution of the host genotype to structuring of bacterial root microbiomes was shown (1, 15, 26, 27) in host species including *A. alpina* (16). Our work suggests that, unlike bacterial communities, root-associated fungal communities are less or not at all affected by host genotypic differences in *A. alpina*. However, we cannot exclude that high within-genotype variability might be shading a small effect.

Soil and Environmental Cues Shape *A. alpina* Root and Rhizosphere Fungal Communities. We next assessed how soil and environment-associated factors shape fungal communities inhabiting bulk soil, the *A. alpina* rhizosphere, and the root endosphere (Fig. 1*A*). Under controlled greenhouse conditions (GrH) we studied the effect of three soils (*SI Appendix*, Table S2) with different geographical origins [Reckenholz (Rec) vs. Lautaret (Lau)] and P-fertilization regimes [Reckenholz soils with amended nitrogen (N) and potassium (K) (RecNK) vs. N, P, and K (RecNPK)]. on the fungal communities associated with *A. alpina* accession Pajares (PM).

Results showed that fungal alpha diversity (related to the number of taxa per sample) estimated by the Shannon diversity index was highly determined by the compartment type ($P = 2.10^{-10}$, 70% of variance, *SI Appendix*, Table S3), with lower values in root relative to rhizosphere and bulk soil compartments (ANOVA and Tukey's HSD, $P < 0.05$) (Fig. 1*C*), indicating the selection of a reduced number of fungal taxa entering the plant roots. Similarly, comparing the structure of those fungal communities (taxa present and their relative abundances) by permutational multivariate analysis of variance (PERMANOVA on Bray–Curtis dissimilarities) revealed that the major source of variation was the compartment type ($P = 10^{-4}$, 29% of variance, *SI Appendix*, Table S3).

Although neither the soil's geographical origin (Reckenholz vs. Lautaret) nor its P-fertilization regime (Reckenholz soils with NK vs. NPK amendment) significantly impacted the overall fungal diversity (ANOVA, $P > 0.05$), they did affect the structure of fungal communities. The effect of the soil's geographical origin (PERMANOVA, $P = 10^{-4}$, 21% of variance) decreased from the bulk soil (67% of variance) over the rhizosphere (49%) to the root compartment (30%), whereas the P-fertilization effect overall was smaller (PERMANOVA $P = 10^{-4}$, 6.3% of variance) and stable across the three compartments (14, 13, and 15% of variance in bulk soil, rhizosphere, and root communities, respectively) (*SI Appendix*, Table S3). This was evident in the PCoA on Bray–Curtis dissimilarities where greenhouse samples from the Lautaret soil (GrH-Lau) were grouped separately from samples obtained from the two Reckenholz soils (GrH-RecNK and GrH-RecNPK), which clustered more closely (Fig. 1*B*). This indicated that, under greenhouse conditions, the compartment type, the soil's geographical origin, and to a lesser extent its fertilization regime, all participated in the shaping of root-associated fungal communities. Collectively, these results suggested that fungal communities that were accommodated in the root endosphere were less diverse and less affected by soil changes than extraradical consortia.

We then assessed whether these fungal communities were affected by the plant growing environment and compared fungal communities established under controlled greenhouse conditions (GrH-Lau) with those established in the common garden under

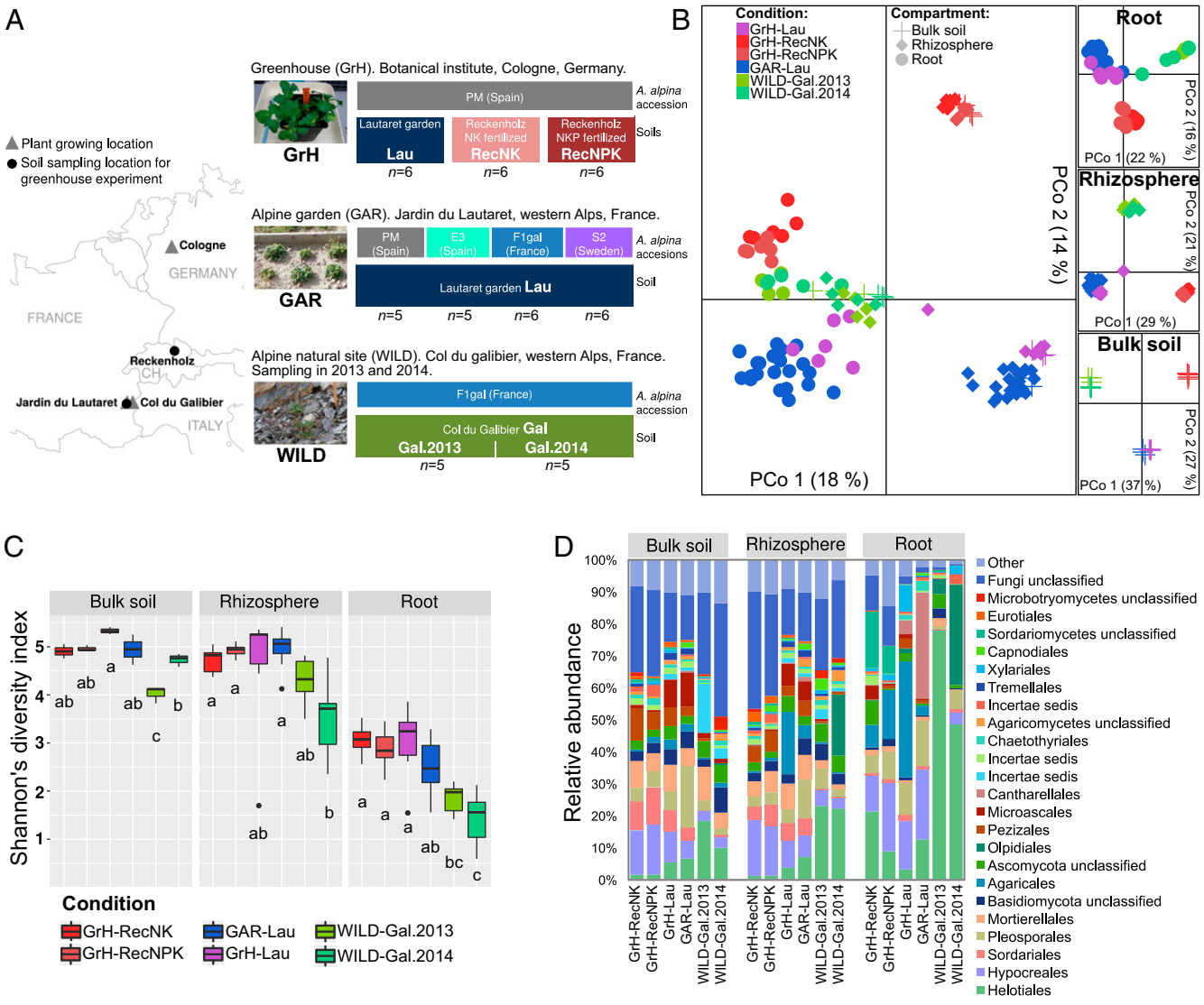

Fig. 1. Comparison of the fungal communities colonizing *A. alpina* roots and rhizosphere under greenhouse (GrH), common garden (GAR), and natural (WILD) conditions in different soils (RecNK, RecNPK, Lau, and Gal). (*A*) Experimental setup showing the different plant growing conditions. The geographic origin of the different *A. alpina* accessions is indicated in parentheses. More information about the soils and the accessions is given in *SI Appendix*, Tables S1 and S2, respectively. The number of biological replicates per condition (*n*) is indicated. (*B*) Principal coordinates analysis on fungal community differences (Bray–Curtis dissimilarities) in the different compartments and conditions. (*C*) Fungal alpha diversity estimated by Shannon's diversity index. Letters a–c indicate significant differences between conditions within each compartment (ANOVA and Tukey's HSD, $P < 0.05$). (*D*) Mean relative abundance of the major fungal orders in the different conditions and compartments: bulk soil, rhizosphere, and root. As the four *A. alpina* accessions studied exhibited similar fungal communities in the garden experiment (*SI Appendix*, Fig. S2), combined results for the four accessions are shown under the "GAR-Lau" condition.

alpine summer conditions (GAR-Lau) in the same soil (Lau) using *A. alpina* PM as host plant. Fungal communities established in the same soil but under the two contrasting environments, i.e., differing in altitude and climate, exhibited similar diversity (ANOVA $P > 0.05$, Fig. 1*C*) but differed in structure (PERMANOVA $P = 0.002$, 10% of variance). The effect of the environment type on fungal community structure increased from bulk soil (PERMANOVA $P = 0.1$) over rhizosphere soil (PERMANOVA $P = 0.002$, 21% of variance) to the root compartment (PERMANOVA $P = 0.003$, 30% of variance) (*SI Appendix*, Table S3). This strongly suggested that root-associated communities were affected to a greater extent by environmental changes than bulk soil communities, which remained largely unaffected.

Comparatively, common garden and wild *A. alpina* plants growing under similar alpine summer conditions but in different soils (GAR-Lau vs. WILD-Gal) also showed differences with lower diversity (Fig. 1*C*) and different community structure (PERMANOVA $P = 10^{-4}$, 20% of variance) in root and rhizosphere fungal communities from wild *A. alpina* (WILD-Gal) (*SI Appendix*, Table S3). This was observable in the PCoA with greenhouse and common garden samples from the Lautaret soil (GrH-Lau and GAR-Lau) clustering close and separating from samples from wild growing *A. alpina* (WILD-Gal) (Fig. 1*B*). Collectively, these results showed that under alpine conditions root-associated fungal communities still diverged according to the soil type.

Stability of Root and Rhizosphere Fungal Communities Across Varying Growth Conditions. We next performed a general analysis including all of the experiments to assess how fungal communities were affected by the plant growing condition. Six plant growing conditions were considered based on the environment and the soil in which the plants grew and included the confounding

effects of two different environments (greenhouse conditions: GrH and alpine summer conditions: GAR and WILD) and four soils (Lau, RecNK, RecNPK, and Gal). Since *A. alpina* accessions harbored similar fungal communities (*SI Appendix*, Fig. S2), samples from the different accessions were grouped under the same plant growing condition, GAR-Lau.

In all plant growing conditions, *A. alpina* root-associated (i.e., root and rhizosphere) fungal communities were dominated by ascomycetes (58% of the fungal reads) belonging mostly to the orders Helotiales, Hypocreales, Pleosporales, and Sordariales. Basidiomycetes (18%), unclassified fungi (14%), zygomycetes (4.4%), and chytridiomycetes (4.1%) were less abundant. As expected for a nonmycorrhizal plant, glomeromycetes that include the AM fungi were rarely detected (0.04%). While the Helotiales (24% of the fungal reads in roots) and Cantharellales (16%) orders were enriched in root samples, Mortierellales (6% of the fungal reads in the rhizosphere), Sordariales (4.2%), and an unclassified basidiomycete taxon (4.1%) were enriched in the rhizosphere (paired *t* test $P < 0.05$) (Fig. 1*D*).

Comparison of fungal communities at the operational taxonomic unit (OTU) level showed again that the compartment type was the main driver of fungal alpha diversity ($P = 2.10^{-16}$, 72% of variance) with a bigger effect than the plant growing condition ($P = 10^{-16}$, 9.4%) (Fig. 1*C*) (*SI Appendix*, Table S3). Comparison of fungal community structure by PCoA showed a separation between root and soil (rhizosphere and bulk soil) samples mainly along the first axis (18% of variance) and a separation between plant growing conditions mainly along the second axis (14% of variance) (Fig. 1*B*). Within the three compartments (root, rhizosphere, and bulk soil) fungal communities clustered according to the geographic origin of the soil: samples from soil Gal (WILD-Gal) separated from soil Lau (independently of the environment) and from Reckenholz soils RecNK and RecNPK, which clustered together (Fig. 1*B*). PERMANOVA analysis indicated that the major source of variation in community structure was the plant growing condition ($P = 10^{-5}$, 32% of variance) and not the compartment type ($P = 10^{-5}$, 16%) (*SI Appendix*, Table S3). This contrasted with the PCoA (Fig. 1*B*), which hinted to a stronger effect of the compartment type. This can be explained by the fact that the PCoA captured only a part of the communities' differences. Interestingly, there was a significant interaction between the compartment type and the plant growing condition (PERMANOVA, $P = 10^{-5}$, 16%, *SI Appendix*, Table S3), suggesting that root, rhizosphere, and bulk soil fungal communities responded differently to varying plant growing conditions. Indeed, PERMANOVA analysis within each compartment showed that the effect of the plant growing condition on the fungal community steadily decreased from the bulk soil ($P = 10^{-5}$, 83%) over the rhizosphere ($P = 10^{-5}$, 59%) to the root ($P = 10^{-5}$, 49%) (*SI Appendix*, Table S3), suggesting that root fungal communities were more robust relative to extraradical assemblages. In sum, this analysis at a wide scale, including contrasting environments and soils, showed that, although the microhabitat type (bulk soil, rhizosphere, or root compartment) is the main driver of fungal alpha diversity, the plant growing condition is the main factor structuring root-associated fungal communities, i.e., determining the taxa present and their abundances. Moreover, it suggested that, compared with rhizosphere communities, fungal communities living within *A. alpina* roots were less affected by changes in the plant growing condition.

Fungal Taxa Consistently Found in *A. alpina* Roots. Following the postulate that commonly occurring organisms play critical roles in their habitat, we aimed at identifying fungal taxa that consistently colonized *A. alpina* roots, hypothesizing that they promote plant growth and/or P uptake. We identified 15 highly conserved fungal OTUs with a high prevalence in roots (i.e., present in at least 85% of the root samples) (Fig. 2*A*). It comprised one zygomycete (*Mortierella elongata*, OTU00045), one basidiomycete (*Ceratobasidiaceae* sp., OTU00008), and 13 ascomycetes belonging to the Helotiales (4 OTUs), the Pleosporales (4 OTUs), the Hypocreales (3 OTUs), the Sordariales (1 OTU), and one unclassified order (OTU00015). On average, this cohort represented 43% of the fungal reads detected in *A. alpina* roots with values ranging from 10 to 93% (Fig. 2*B*). Of these 15 highly conserved root OTUs, 7 were enriched in plant roots in comparison with the rhizosphere (paired *t* test, $P < 0.05$). They included two unclassified species belonging to the Pleosporales (OTU00007, 92% prevalence, 1.1% relative abundance) and the Ceratobasidiaceae (OTU00008, 90%,

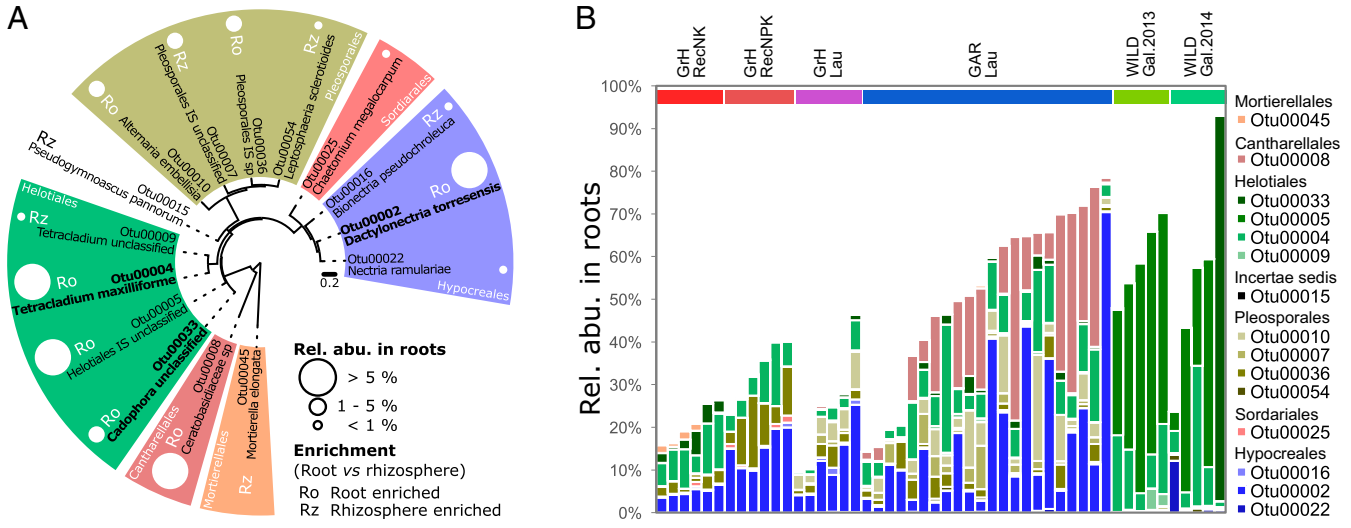

Fig. 2. Fungal taxa consistently found in *A. alpina* roots (>85% prevalence across all root samples). (*A*) Maximum-likelihood phylogenetic tree of the highly conserved root OTUs. The representative ITS2 sequences from the OTUs were aligned using Muscle (28) and used for tree inference in PhyML (29) with a GTR+I+γ model with optimized parameters. Fungal orders are depicted with different colors; white circles indicate the average relative abundance (Rel. abu.) of the OTU in root samples. Root (Ro)- or rhizosphere (Rz)-enriched OTUs are indicated (comparison root vs. rhizosphere relative abundance, paired *t* test, $P < 0.05$). OTUs with 100% prevalence are shown in boldface type. (*B*) Relative abundance of the 15 highly conserved root OTUs in each root sample. The data are given in Dataset S4.

6.5%); *Alternaria embellisia* (OTU00010, 88%, 2.8%); *Dactylonectria torresensis* (OTU00002, 100%, 11%); and three Helotiales including *Tetracladium maxilliforme* (OTU00004, 100%, 8.5%), a *Cadophora* OTU (OTU00033, 98%, 3%), and an unclassified OTU (OTU00005, 86%, 7%) (Fig. 2*A*). None of these highly conserved root OTUs was related to (*i*) AM, ectomycorrhizal, or orchid mycorrhizal fungi known to facilitate plant nutrient uptake or to (*ii*) fungal endophytes *S. indica* (syn. *P. indica*) or *C. tofieldiae*, which were described to transfer P to nonmycorrhizal plants. Four of these OTUs belonged to the Helotiales order known to encompass ericoid mycorrhizal fungi such as *Oidiodendron maius* but also plant pathogens such as *Rhynchosporium secalis*. Three of these four Helotiales OTUs showed enrichment in roots and high abundance especially under natural conditions (Fig. 2*B*).

Helotiales Fungus F229 (OTU00005) Promotes *A. alpina* Growth and Shoot P Accumulation. Helotiales OTU00005 exhibited a high relative abundance in the roots of wild *A. alpina* plants from Col du Galibier (45% in WILD-Gal.2013 and 23% in WILD-Gal.2014 samples, *SI Appendix*, Fig. S5*B*), where the host plants grew on an extremely low-P soil (soil Gal, 3.7 mg/kg plant-available P) while maintaining high shoot P concentration (*SI Appendix*, Fig. S5*A*). We subsequently identified in our Cologne Culture Collection of Root-Associated Fungi (CORFU) seven isolates that were recovered from *A. alpina* collected at Col du Galibier and belonged to this OTU (Dataset S1). The full-length ITS sequences of the isolates shared 99–100% similarity, and their ITS2 regions showed 99–100% similarity to the representative ITS2 sequence of OTU00005. Blast analysis revealed that the ITS sequences of these isolates were highly similar to other Helotiales root endophytes isolated from the Brassicaceae species *Microthlaspi perfoliatum* growing in the south of Spain (30), thus reflecting a recurrent presence of these Helotiales fungi in roots of Brassicaceae (*SI Appendix*, Fig. S3).

To address the significance of fungal root colonization for plant P uptake, the fungus with CORFU identifier F229 (hereafter named F229), belonging to OTU00005, was selected for further in planta experiments in gnotobiotic Murashige and Skoog (MS) agar systems. F229 promoted growth of *A. alpina* F1gal and PM roots under low-P conditions and left plants unaffected in high-P conditions (*SI Appendix*, Fig. S4). In contrast, another six fungal isolates not belonging to OTU00005 (CORFU F226, F248, F247, F91, F83, F222), screened in different experiments, all exerted a negative effect on plant root and/or shoot growth in at least one of the P conditions (*SI Appendix*, Fig. S4). Fourteen days post-inoculation (dpi) on its natural host *A. alpina* F1gal, F229 asymptomatically colonized the plant roots (*SI Appendix*, Fig. S6 *B* and *C*) with equal colonization at low-P (100 μM P MS agar, 89.6% of colonized roots) and high-P (1,000 μM, 88.6% of colonized roots) conditions (χ^2 test $P = 0.87$). However, under low-P conditions, fungal inoculation significantly increased root length (+12%, *t test* $P = 0.02$) and root surface area (+19%, *t* test $P = 0.001$) while leaving shoot biomass (*t* test $P > 0.05$) and shoot P concentration (*t* test $P > 0.05$) unchanged (*SI Appendix*, Fig. S6 *A* and *B*). A neutral effect on root growth was apparent under high-P conditions (1,000 μM P, 14 dpi) (*SI Appendix*, Fig. S6*A*). Similarly, a second isolate (CORFU F240), also assigned to OTU00005 and exhibiting 100% ITS sequence similarity with F229, also promoted root growth of *A. alpina* F1gal under low-P conditions (*SI Appendix*, Fig. S6*D*).

We next assessed the effect of F229 on the growth of its natural host *A. alpina* F1gal under native P-limited soil conditions (Fig. 3*A*). At 28 dpi in gnotobiotic microcosms filled with autoclaved soil from the Col du Galibier (soil Gal), F229 fully colonized plant roots (100% of colonized roots) inter- and intracellularly (Fig. 3*B*, *a*–*d*). Vital staining of plant and fungal membranes indicated viability of host and fungal cells during intracellular accommodation (Fig. 3*B*, *d*), indicating a biotrophic interaction between the partners. While addition of heat-killed fungal suspension negatively affected plant growth, fungal inoculation translated into 52% higher shoot biomass (Mann–Whitney test $P = 3.10^{-13}$) and

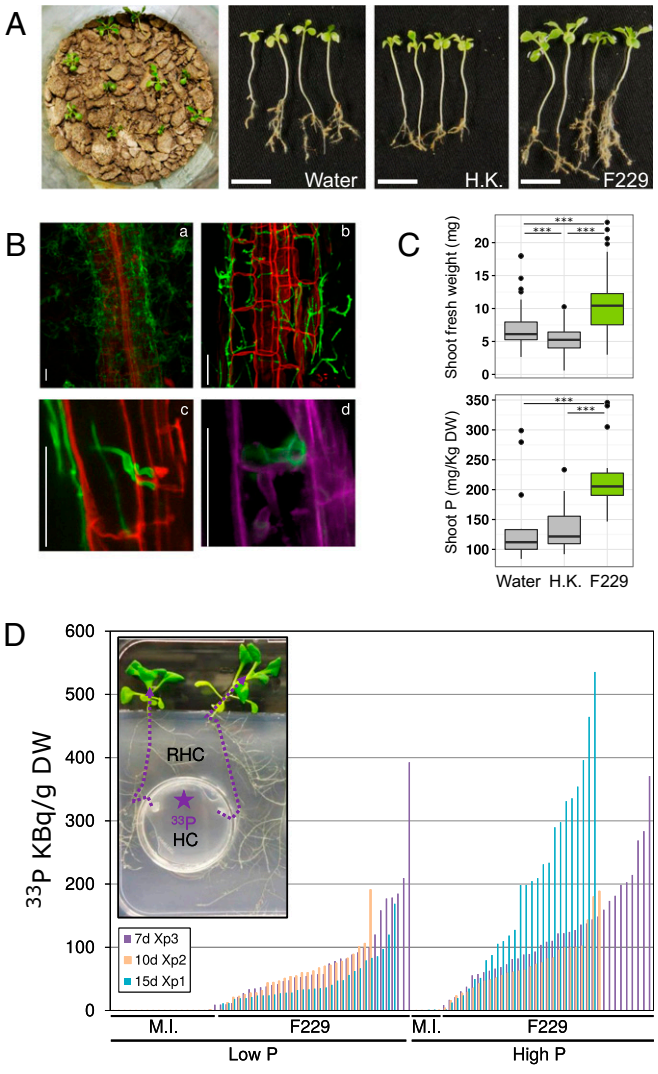

Fig. 3. Fungus F229 (OTU00005) increases *A. alpina* growth and P content under native low-P soil conditions and is capable of hyphal P transfer to the root in vitro. (*A*) *A. alpina* F1gal growth in sterile soil microcosm upon water addition (Water), addition of heat-killed fungus (H.K.), and inoculation with F229 (F229) ($1.32 \pm 0.8 \times 10^4$ propagules per microcosm) at 28 dpi. (Scale bars, 1 cm.) (*B*) Inter- and intracellular fungal root colonization in sterile soil microcosms visualized by confocal microscopy after staining the fungal cell wall with WGA-Alexa (green, *a*–*d*), the plant cell wall with propidium iodide (red, *a*–*c*), and the cellular membranes with FM4-64 (purple, *d*). (Scale bars, 30 μm.) (*C*) Effect of F229 inoculation on shoot fresh weight and shoot P concentration in sterile soil microcosms. The experiment was repeated four times including the Water and F229 treatments and three times including also the H.K. treatment, with three to four microcosms per treatment; similar results were obtained, and compiled results from the four experiments are shown here. Shoot weight was measured on individual plants ($n \geq 56$) whereas all of the shoots from one microcosm were pooled to measure shoot P content by ICP-MS ($n \geq 9$). Asterisks indicate significant differences between the treatments based on the Mann–Whitney test ($P < 0.05$). (*D*) In vitro transfer of ^{33}P orthophosphate to the plant by F229. The F229 and *A. alpina* F1gal plants were grown on low-P (100 μM P) or high-P (1,000 μM P) MS medium in a two-compartment system. ^{33}P was added to the fungal HC, and after 7 (experiment 3), 10 (experiment 2), or 15 (experiment 1) days, ^{33}P incorporation into the plant shoot growing in the RHC was measured by scintillation counting of individual plants. No fungus was added to the fungal compartment in the mock inoculated treatments. Bars represent individual samples.

61% higher shoot P concentration (Mann–Whitney test $P = 2.10^{-4}$) compared with the water control (Fig. 3*C*). The shoot P levels were still lower than observed in their wild-growing counterparts (WILD-Gal treatments, *SI Appendix*, Fig. S5). We could imagine two possible reasons explaining this discrepancy: (*i*) The young plants in the microcosms accumulated less P in their vacuoles, the primary intracellular compartments for inorganic phosphate, than the much older wild plants or (*ii*) differences in properties of soil in microcosms relative to soil at Col du Galibier limited P uptake, which was partially alleviated through root colonization with F229. In sum, these results corroborate the hypothesis of a beneficial effect of this endophyte on host growth and P acquisition under native low-P soil conditions.

F229 Translocates P to Its Host in Vitro. Fungi can promote plant P acquisition by different mechanisms like P solubilization, P mineralization, or hyphal P transfer. We wanted to know whether F229 is capable of hyphal transport of radiolabeled ^{33}P to its host. Using a two-compartment agarose system limiting radiotracer diffusion, we observed that ^{33}P added to the hyphal compartment (HC) could be traced to the plant shoot in the root and hyphal compartment (RHC), with both compartments connected only by fungal hyphae crossing the physical barrier (Fig. 3*D*). Fungal colonization was restricted to the root as the fungus was never detected in the plant shoot (stem or leaves, *SI Appendix*, Fig. S7). ^{33}P translocation across the diffusion barrier was blocked by Benomyl (*SI Appendix*, Fig. S8), a compound that inhibits microtubule formation and intracellular transport in fungi (31), which indicated that hyphal P transport was an active fungal process rather than mediated by diffusion. Moreover, hyphal ^{33}P translocation to the plant shoot was detectable as early as 7 d after ^{33}P addition and was independent from low- or high-P conditions. This suggests that in F229 ^{33}P transfer to the host is not regulated by P availability, which stands in contrast to what was shown for *C. tofieldiae* (12). These data suggest that plant growth promotion by F229 under low-P soil conditions involves hyphal transfer of P into its host.

The F229 Genome Encodes Two High-Affinity Phosphate Transporters. Cellular uptake of nutrients, maintenance of cellular nutrient homeostasis, and ion transfer across cellular (endo)membranes in fungus–plant symbioses involves high- and low-affinity ion transporters. To obtain insight into the molecular mechanisms underlying transport of inorganic phosphate in F229, we performed genome-wide analysis to identify fungal phosphate transporters. PacBio sequencing of the F229 genome produced a final assembly of 39 contigs with an estimated genome size of ∼85 Mb (Dataset S2). The final genome version showed a high level of completeness with a high coverage of core fungal (98.7%, FUNYBASE gene set) and eukaryotic genes (99.2%, Cluster of Essential Genes gene set). We aimed to identify homologs of six proteins that play a role in phosphate transport in the yeast *Saccharomyces cerevisiae*. One is the major proton-coupled high-affinity phosphate transporter Pho84, three transport phosphate with low affinity into cells (Pho87, Pho90, Pho91), and the fifth and sixth proteins (Pho 88 and Pho89) are utilized under specialized conditions (32). Two genes in the F229 genome (g8711.t1 and g16086.t1) encode proteins sharing high similarity with *S. cerevisiae* Pho84 and with fungal high-affinity phosphate transporters involved in P translocation from fungus to plant. One gene (g3490.t1) encodes a protein sharing similarity with Pho87, Pho90, and Pho91, and a last gene (g6261.t1) encodes a protein sharing similarity with Pho88. The gene encoding the Na^+-dependent high-affinity Pho89 could not be identified (*SI Appendix*, Fig. S9). In sum, these results show that the F229 genome encodes a set of phosphate transporters potentially enabling phosphate uptake and translocation to its host plant.

The Endophytic Lifestyle of F229 is Associated with the Expansion of its CAZyme Repertoire. We aimed at identifying genomic characteristics associated with the F229 endophytic biotrophic lifestyle. A five-gene phylogenetic analysis on F229 and 50 other ascomycetes with available genome information confirmed the placement of the fungus within the Leotiomycetes class and the Helotiales order (*SI Appendix*, Fig. S10). The classification of the fungus at the family or genus level was not possible as the taxonomy within the Helotiales order is still unclear. The closest relatives (with sequenced genome) of F229 are plant pathogens *Marssonina brunnea* f. sp. *multigermtubi* and *Rhynchosporium* species *R. secalis*, *R. commune*, and *R. agropyri*, suggesting that the endophytic lifestyle of F229 could have evolved from an ancestral plant pathogenic lifestyle (Fig. 4*A*). Similarly, the ITS-based phylogenetic analysis including more fungal isolates suggests that F229 belongs to a lineage of root endophytic fungi that diverged from related pathogenic *Rhynchosporium* and *Pyrenopeziza* species (*SI Appendix*, Fig. S3), but more Helotiales genomes are needed to properly assess this hypothesis using more robust phylogenetic analyses.

The Helotiales order encompasses fungi with contrasting lifestyles including plant beneficial fungi, plant pathogens, and saprotrophs (Fig. 4*A*). We used a comparative genomics approach on CAZyme repertoires to identify genomic signatures associated with a biotrophic lifestyle and plant-beneficial effects within this order. Comparison of CAZyme class profiles of 11 Helotiales fungi revealed large similarities between plant beneficial fungi that clustered together (Fig. 4*B*). The cluster including F229, the poplar endophyte *Phialocephala scopiformis*, and the ericoid mycorrhiza *O. maius* was characterized by a higher number (*t* test $P < 0.01$) of modules of glycoside hydrolases (GH) (average number of 427 in plant-beneficial fungi, 349 in F229, and 256 in the other fungi), carbohydrate-binding modules (CBM) (103, 109, and 77), carbohydrate esterases (CE) (194, 160, and 105), glycosyltransferases (GT) (128, 122, and 102), and auxiliary activities (AA) (137, 135, and 83), indicating an overall larger CAZyme repertoire in the genomes of plant beneficial Helotiales in comparison with plant pathogenic and saprotrophic Helotiales (Dataset S3). Comparison of CAZyme family profiles showed similar results (*SI Appendix*, Fig. S11). Twenty-two CAZyme families were significantly more abundant in plant beneficial fungi in comparison with the other fungi (*t* test $P < 0.01$) (Fig. 4*C*). Notably, this concerned families associated with plant cell-wall degradation, acting on hemicellulose (GH31, GH29, CE1, CE7, CE10), or in the transformation of lignocellulosic compounds (AA7). Three GHs associated with fungal cell-wall degradation (GH20, GH72, GH76) were also more abundant in plant beneficial fungi. Comparison of CAZyme classes (*SI Appendix*, Fig. S12*A*) and selected CAZyme families (*SI Appendix*, Fig. S12*B*) across 51 ascomycetes genomes showed no clustering corresponding to fungal lifestyle differences, indicating that the observations made within the Helotiales are lineage-specific. Collectively, these data suggest that the endophytic behavior of F229 is associated with the enlargement of its CAZyme repertoire and particularly with protein families associated with plant cell-wall degradation.

Discussion

Low availability of phosphate is a major factor constraining plant growth, performance, and metabolism in many natural and agricultural soils worldwide due to the poor solubility and mobility of soil P. The AM fungi have been shown to benefit plant productivity due to their contribution to plant nutrition, especially in nutrient-poor soils (10). The predominant function of AM fungi is attributed to increased host plant phosphate uptake as a consequence of a phosphate transport mechanism (7). Brassicaceae species lack the ability to establish an AM symbiosis, and, to fully comprehend how these plants thrive in P-limited habitats, it is required that we improve our understanding of their

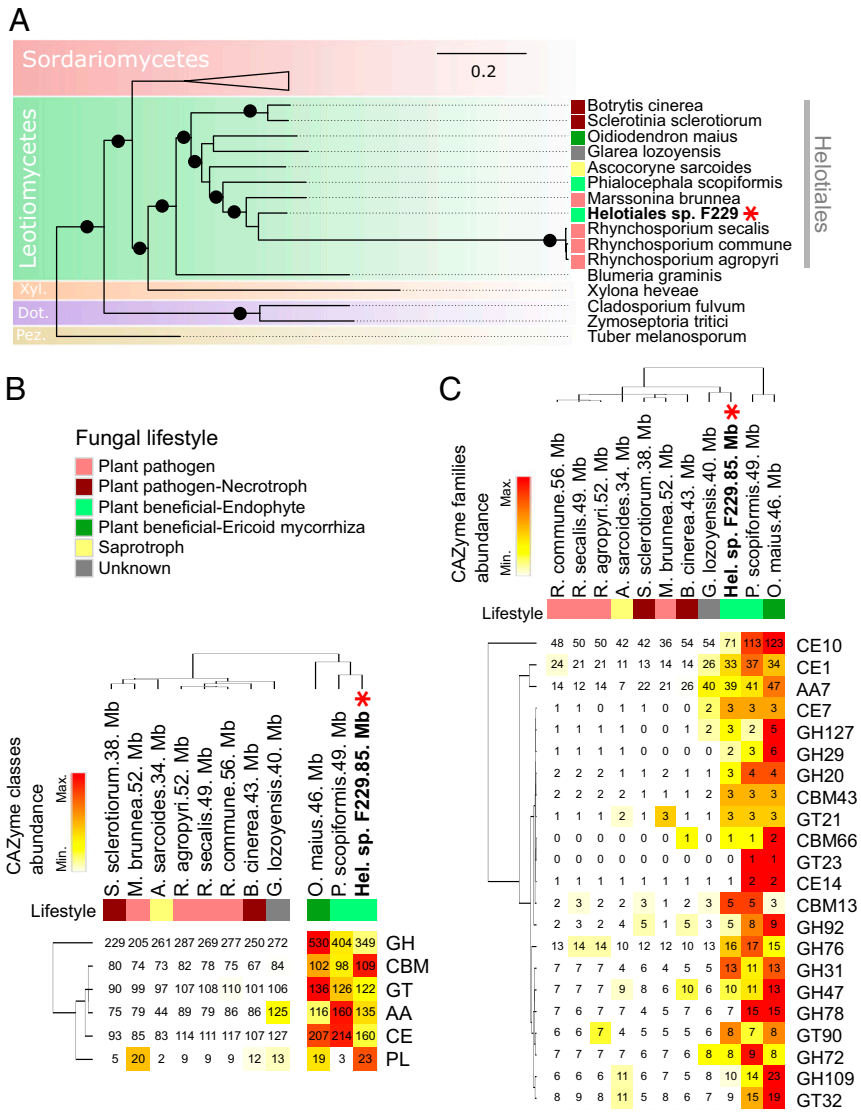

Fig. 4. The endophytic lifestyle of F229 is associated with the expansion of its CAZyme repertoire. (*A*) Maximum-likelihood phylogenetic tree inferred from five housekeeping genes (28S, 18S, Rpb1, Rpb2, EF1alpha). Bootstrap values >0.75 are indicated with a black dot. *Laccaria bicolor* sequences were used for tree rooting. Helotiales with plant beneficial, plant pathogenic, or saprophytic lifestyles are indicated; the key is given in *B*. The full tree is shown in *SI Appendix*, Fig. S10. (*B*) Comparative analysis of CAZyme repertoires in the genome of F229 and related Helotiales with plant beneficial, plant pathogenic, or saprophytic lifestyles. Hierarchical clustering on the abundance of CAZyme classes within the Helotiales. AA, auxiliary activities; CBM, carbohydrate-binding module; CE, carbohydrate esterase; GH, glycoside hydrolase; GT, glycosyltransferase; PL, polysaccharide lyase. (*C*) Hierarchical clustering on the abundance of selected CAZyme families within the Helotiales. Only families showing a significantly higher abundance in plant-beneficial fungi are shown (*t* tests, $P < 0.01$). In *B* and *C*, the color scale depicts standardized values for each module. Fungal genome sizes are indicated after their name. F229 is shown in boldface type with an asterisk.

fungal microbiota. Here we close this gap by investigating structural and functional properties of the fungal microbiota associated with the roots of the nonmycorrhizal Brassicaceae species *A. alpina*. We have chosen *A. alpina* because it naturally grows in low-P habitats, and, in contrast to short-lived annuals like the model species *A. thaliana*, its perennial pattern of growth and development gives longer time periods for microbial communities to establish in and around the roots.

Variability and Stability of the *A. alpina* Root Fungal Microbiome. Our study of the factors shaping root-associated fungal communities showed that fungal alpha diversity is determined mainly by the microhabitat type, i.e., bulk soil, rhizosphere, or root compartment, dropping dramatically in the root (Fig. 1*C*). This observation further sustains the view that colonization of the root endosphere is restricted to a reduced number of fungal taxa that have the ability to cross the selection filters imposed by the host. This hypothesis is supported by previous studies on root microbial communities that have shown a similar diversity pattern in bacterial assemblages in *A. alpina*, *A. thaliana*, and rice (1, 15, 16, 26) and in fungal communities of *Agave* (20). Furthermore, the microhabitat type also affected the structure of these fungal communities, i.e., the taxa present and their relative abundances (Fig. 1*B*). Overall, the fungal microbiome associated with roots (root and rhizosphere) of nonmycorrhizal *A. alpina* was dominated by ascomycetes, as was shown for mycorrhizal poplar and *Agave* (18, 20), and which is likely to be predetermined by the majoritarian presence of ascomycetes in soil (33). Still, root endosphere communities systematically differed from rhizosphere communities located millimeters apart (Fig. 1*B*); they were enriched in Helotiales and Cantharellales fungi and depleted in Mortierellales and Sordariales (Fig. 1*D*). Surprisingly, there was no clear similarity in

the pattern of enriched and depleted fungal orders in *A. alpina* and mycorrhizal *Agave*, poplar, and sugarcane roots (18–20), suggesting a low level of conservation of fungal microbiome patterns across distantly related plant host species.

Adding to the strong microhabitat effect, the soil geographical provenance was the second largest driver of fungal community structure under controlled greenhouse conditions. Soil fungal communities show strong biogeographical patterns shaped by local climatic and edaphic factors (33–35) and thus strongly diverge from the "everything is everywhere" postulate suggested for microbial communities (36). The soil's P-fertilization regime also impacted the structure of fungal communities, albeit to a lesser extent than the soil geographical origin (Fig. 1*B*). This indicated that long-term P fertilization of the RecNPK soil (37) shifted soil fungal communities. Differences in root communities could be the consequence of these changes, but we cannot exclude that they could be linked to changes in the plant nutritional status associated with fertilization. Such changes could lead to differences in root-associated communities by altering the root exudation profile and/or morphology, similarly to the AM symbiosis that is confined to conditions in which the plant is P-starved (7, 37). Even when growing in the same soil, fungal communities described under controlled greenhouse conditions differed from those established under alpine summer conditions (Fig. 1*B*). This environment effect increased from the bulk soil to the root compartment, suggesting that root-associated communities were more responsive to environmental change than bulk soil communities, which remained roughly alike. Low night temperatures (prevalent under alpine summer conditions) affect plant defense mechanisms as shown in *Arabidospsis* (38), which could directly impact endophytic fungal communities.

Our analysis including all of the plant growing conditions studied showed that at this wide scale it was no longer the microhabitat type, i.e., the compartment type, but the plant growing condition that was the main factor shaping fungal communities. This is consistent with what has been described in *Agave* (20) and poplar (18), where the plant biogeography was the major source of variation in fungal and bacterial communities. Interestingly, root communities were less affected by the plant growing condition than soil communities (rhizosphere and bulk soil) (Fig. 1*B*) as observed in *Agave* (20). This pointed to the existence of a set of fungal taxa consistently colonizing *A. alpina* roots in contrasting growth conditions. Our study revealed a highly conserved set of 15 OTUs that was dominated by ascomycetes (Fig. 2*A*) and represented up to 93% of the fungal reads in *A. alpina* roots (Fig. 2*B*). Seven OTUs of this core microbiome were significantly enriched in the root endosphere in comparison with the rhizosphere (Fig. 2*B*), suggesting not only that these taxa were able to cross the selection barrier imposed by the root, but also that they reached a higher abundance within the root endosphere, implying some degree of adaptation to this niche. Although most of the identified OTUs could not be classified at the species level, we could identify the *A. embellisia* and *D. torresensis* species. Both *Alternaria* and *Dactylonectria* genera are known to contain a high number of plant pathogenic species albeit with no evidence of pathogenicity in *A. alpina*. Interestingly, three closely related Helotiales OTUs were identified as highly conserved, root-enriched, and highly abundant in wild-growing plants (Fig. 2*A*). While Helotiales fungi represented 24% of the *A. alpina* root microbiome, they were not commonly found in root microbiomes of the mycorrhizal hosts *Agave* (20), poplar (18), or sugar cane (19). However, they were found to dominate the root microbiome of mycorrhizal Ericaceae species growing under similar cold and nutrient-limited conditions as *A. alpina* (39), suggesting that this could be a specificity of plants growing in such harsh environments. The Helotiales order is not well studied, and its phylogeny is still obscure. Although Helotiales fungi have often been isolated from plant roots, their ecological functions remain largely unknown (40). Our results indicating a plant growth-promoting effect of two Helotiales isolates (F229 and F240, OTU00005) in vitro (*SI Appendix*, Fig. S6) in combination with the high relative abundance of the corresponding OTU in *A. alpina* plants growing under P-poor natural conditions (*SI Appendix*, Fig. S5) suggests that this taxon could facilitate plant P uptake in its natural environment. Further studies are needed to investigate more *A. alpina* natural populations at different locations to define the biogeographic distribution of this beneficial plant–fungus association.

Endophytic Helotiales Fungus F229 Promotes Growth and P Acquisition in *A. alpina*. While most root-associated microbes compete with the plant and with each other for essential nutrients, some may have the potential to positively affect plant nutrition and growth. Helotiales fungal isolate F229 belonging to OTU00005 was isolated from *A. alpina* roots growing at the Col du Galibier natural site characterized by low-P availability in soil. The fungus exhibited biotrophic endophytic growth as it asymptomatically colonized plant roots inter- and intracellularly (Fig. 3*B*) rather than killing root cells during the infection process, coinciding with the root enrichment of the corresponding OTU (Fig. 2*A*). F229 was able to translocate P to the plant under high- and low-P conditions on MS agar (Fig. 3*D*). However, no increase in shoot P content was observed under those conditions (*SI Appendix*, Fig. S6). One plausible explanation is that as observed for AM symbiosis, translocation of P by the fungus does not necessarily translate into increased P content in the plant since the plant can tune-down the direct P uptake pathway and use the mycorrhizal pathway instead (41). When reintroduced into its native low-P soil fungus, F229 successfully colonized plant roots and enhanced shoot growth and shoot P concentration (Fig. 3*C*) through an active process (Fig. 3*C*). Our results stay in accordance with a role of F229 in extending the potential range of plant nutrient absorption in low-P soils and potentially also in P-rich habitats. In addition to increasing the absorptive surface area of the host plant root system, hyphal P translocation mediated through the activity of phosphate transporters encoded in the fungal genome would enable access to soil P sources otherwise unavailable to the plant (Fig. 3*D* and *SI Appendix*, Fig. S9). We cannot exclude, however, P delivery from fungus to host as a consequence of lysis of fungal cells, a mechanism that was proposed for nutrient transfer in orchid mycorrhizae (42). Overall, our work on F229 (P transfer) and studies on *S. indica* (P transfer) (13, 14), *C. tofieldiae* (P transfer) (12), *Heteroconium chaetospira* (N transfer), (43) and *Metarhizium robertsii* (N transfer) (44) provide accumulating evidence that fungus-to-plant nutrient transfer, generally assigned to classical mycorrhizal symbioses (10), is more common than previously thought.

Plant-colonizing fungi rely on hydrolytic enzymes including CAZymes for degradation of the plant cell wall and penetration into the host tissue (45, 46), and changes in the CAZyme repertoires have been associated with lifestyle changes in plant-associated fungi (21, 22). The evolution from pathogenic ancestors toward the beneficial endophytic lifestyle of F229 was accompanied by the enlargement of its CAZyme arsenal (Fig. 4). This contrasts with observations of ectomycorrhizal fungi where the transition from a saprophytic to an endophytic lifestyle was associated with a reduction of the number of genes encoding plant cell-wall–degrading enzymes (21, 22). This discrepancy has been noted in other root endophytes including mycorrhizal fungi (21, 45, 47). One explanation is that the arsenal of enzymes potentially involved in plant cell-wall degradation is a genomic indicator of saprophytic growth in plant debris in soil, making these fungi less dependent on their host for photosynthetically derived carbon.

In conclusion, by studying the fungal microbiota associated with *A. alpina* roots, we have uncovered a beneficial Helotiales fungus capable of promoting plant growth and P uptake and thereby potentially facilitating plant adaptation to low-P environments.

Materials and Methods

Plant Growth and Sample Collection. We analyzed the fungal communities colonizing the roots and rhizosphere of 60 *A. alpina* plants growing (*i*) under GrH in three different soils (Lau, RecNK, and RecNPK; soil characteristics are given in *SI Appendix*, Table S2); (*ii*) under alpine summer conditions in a common garden in the French Alps (GAR); and (*iii*) at a natural site in the French Alps (WILD) over 2 y (2013 and 2014) (Fig. 1*A*). Four *A. alpina* accessions (PM, E3, S2, and F1gal) originating from different European locations with different soil characteristics (*SI Appendix*, Table S1) were included in the common garden experiment to assess the contribution of the plant genotype to the structuring of the root-associated fungal community. Root and rhizosphere compartments from five to six replicates per condition were collected. The rhizosphere was sampled as the soil tightly adhering to roots, and root samples were enriched in endophytic fungi by detaching surface-adhering fungi through sonication (1). Three unplanted bulk-soil samples were included in each experiment. The detailed procedure is given in *SI Appendix, Materials and Methods*. In each treatment, surface-sterilized roots were used to recover fungal root endophytes deposited in CORFU (Dataset S1). The method is described in *SI Appendix, Materials and Methods*.

Shoot P Measurements by Inductively Coupled Plasma Mass Spectrometry. For determination of shoot P concentration by inductively coupled plasma mass spectrometry (ICP-MS), shoot samples were dried for 2 d at 65 °C before digestion. For mature plants (i.e., ∼3 mo old; GrH, GAR, and WILD experiments), samples were digested using a microwave system (Multiwave 3000; Anton Paar). Approximately 0.3 g of dry homogenized plant material was digested using 4 mL of HNO_3 (66% vol/vol) and 2 mL of H_2O_2 (30% vol/vol). The microwave program included a power ramp of 10 min followed by 30 min at 1,400 W and a final 15 min of cooling down. Final solutions were diluted 1:5 with deionized water before analysis. For young plants (i.e., 1 mo old; MS agar and sterilized soil experiments) plant material was digested using 500 μL of HNO_3 (66%) at 100 °C for 20 min. Final solutions were diluted 1:10 with deionized water before analysis. Solution blanks were included. The P concentration was determined using an Agilent 7700 ICP-MS (Agilent Technologies) following the manufacturer's instructions.

Fungal Microbiome Analysis. For fungal community description, DNA was extracted from each compartment, i.e., root, rhizosphere, and bulk soil, and used for fungal ITS2 PCR amplification with primers ITS9/ITS4 (*SI Appendix*, Table S4). Tagged amplicons were sequenced using an Illumina Miseq platform producing 2 × 300 paired-end reads, and data analysis was conducted in Mothur (48). The final 3′388.918 high-quality fungal reads were clustered using de novo OTU picking at 97% sequence similarity. After discarding low abundance (<50 reads) and nonfungal OTUs, 2.966 OTUs were obtained, and each OTU was taxonomically classified using the UNITE database in Mothur. On average, 38.405 final fungal reads and 567 OTUs were obtained per sample (*SI Appendix*, Table S5). Highly conserved root OTUs (>85% prevalence across all root samples) are given in Dataset S4. The detailed procedure is given in *SI Appendix, Materials and Methods*. The raw sequencing data have been deposited at the National Center for Biotechnology Information (NCBI) Short Read Archive under Bioproject PRJNA386947.

Statistical Methods Used for Microbiome Studies. Analyses were conducted in R 3.2.3. The OTU relative abundances were calculated and transformed using a $\log_{10}(x + 1)$ formula. Bray–Curtis dissimilarities between samples were calculated using the "vegdist" function of the vegan package (49) and used for principal coordinates analysis using the "dudi.pco" function of the ADE4 package (50). Fungal alpha diversity was estimated in each sample using the Shannon diversity index (H) calculated in Mothur. Means were compared with ANOVA followed by Tukey's HSD ($P < 0.05$). PERMANOVA on Bray–Curtis dissimilarities was conducted to study the effect of different factors on the structure of fungal communities using the "Adonis" function of the vegan package (at $P < 0.05$). As previously performed in a study on metal bioaccumulation in plants (51), we calculated a P-accumulation factor (P concentration in the plant shoot divided by the plant-available P concentration in the soil). Plant-available P in the soil (*SI Appendix*, Table S2) was measured using the ammonium-acetate EDTA extraction method (AAE10) by the Laboratory for Soil Analysis (Thun, Switzerland), and shoot P was measured by ICP-MS as indicated above.

Effect of F229 Inoculation on *A. alpina* Growth in Sterile-Soil Microcosms. For sterile-soil microcosms, 250 g of soil Gal (low plant-available P: 3.7 mg/kg, *SI Appendix*, Table S2) was put into 500-mL glass jars (Weck) and autoclaved twice with a 48-h interval. Since fungus F229 did not sporulate under our experimental conditions, a mycelium suspension was used for inoculation. After growing the fungus for 4 wk on malt yeast peptone agar, the fungal mycelium was recovered from the surface of the agar, weighted, and diluted to 250 mg/mL with sterile water, and ∼30 glass beads per milliliter (Ø 1.7–2.1 mm) (Carl Roth) were added before grinding twice at 6,200 × *g* for 10 s in a Precellys instrument (Bertin Technologies). The mycelium was subsequently washed twice through addition of nine volumes of water and centrifugation at 700 × *g* for 2 min. The final pellet was resuspended in sterile water, and the mycelial concentration was adjusted to 10 mg/mL. Fungus-treated microcosms were inoculated with 10 mL of this inoculation suspension (100 mg of mycelium per pot), heat-killed controls received 10 mL of this suspension after autoclaving, and water controls received 10 mL of sterile water. Plate dilution series were made with the inoculum suspension, and colony counting after 4 d indicated a level of inoculation of $1.32 \pm 0.8 \times 10^4$ propagules per pot. Soil humidity was adjusted to 70% of the water-holding capacity without further watering. *A. alpina* F1gal seeds were surface-sterilized as described in *SI Appendix, Materials and Methods*, and stratified for 1 wk at 4 °C on moist sterile filter paper, and 10 seeds were subsequently placed on the soil surface in each microcosm 2 d after fungal inoculation. The microcosms were closed and placed in a phytochamber (Versatile Environmental Test Chamber; Sanyo) with 16-h/8-h day/night cycles at 22/18 °C and 70% relative humidity. The microcosms were randomized every other day. After 28 d, plants were harvested individually, shoot weight was measured, and all of the shoots from one microcosm were pooled to measure shoot P content by ICP-MS as described above. One root system per microcosm was collected for microscopy analysis of fungal colonization. Microscopy analyses were conducted as described in *SI Appendix, Materials and Methods*. The experiment was repeated four times; three experiments included the "heat-killed"' treatment, with three to five microcosms per treatment. Due to a reduced germination rate, on average seven plants per microcosm could be sampled ($n = 10–39$ per treatment per experiment). Data normality was checked, and means were compared with the Mann–Whitney test ($P < 0.05$). The impact of fungal inoculation on *A. alpina* growth was also studied on MS agar; the detailed procedure is given in *SI Appendix, Materials and Methods*.

^{33}P Translocation Experiments. In vitro hyphal transfer of ^{33}P orthophosphate to the plant by F229 was studied as described in ref. 12. A bicompartment system was established by placing two small round petri plates (Ø 3.8 cm) constituting the HC into a square petri plate that was filled with low-P (100 μM P) or high-P (1,000 μM P) MS agar up to the rim of the small plate, which served as the RHC. Roots were precluded from growing into the HC by regularly moving root tips before root ingrowth, thus maintaining the physical barrier between both compartments (Fig. 3*D*). Four-week-old fungal potato dextrose agar plates were used to inoculate the HC by transferring a 0.5-cm^3 agar plug containing fungal hyphae. *A. alpina* F1gal seeds were surface-sterilized, stratified, and allowed to germinate on low-P MS agar as described in *SI Appendix, Materials and Methods*. After 2 wk of fungal growth in the bicompartment system, two 1-wk-old *A. alpina* F1gal seedlings were transferred to the RHC. No fungus was added to the HC in the mock treatments. Plates were closed with Micropore tape, placed vertically in a phytochamber (Sanyo, 16 h/8 h day/night cycles at 22/18 °C and 70% relative humidity), and incubated for another 2 wk. When fungal hyphae had crossed the physical barrier between both compartments, 350 kBq of carrier-free ^{33}P-labeled H_3PO_4 (∼3 pmol; Hartmann Analytik) was added to the HC. Plates were incubated horizontally in the phytochamber, and after 7 (experiment 1), 10 (experiment 2), or 15 d (experiment 3), plant shoots were sampled, dried overnight at 65 °C, digested with 500 μL 66% HNO_3 at 100 °C for 20 min with addition of 250 μL H_2O_2, and heated at 100 °C for 1 min. The solution was diluted 1:10, and 500 μL was mixed with 4.5 mL of scintillation mixture (Rotiszint eco plus; Roth) and used for detection of ^{33}P signals with a scintillation counter (Beckman Coulter LS 6500). Between 5 and 36 plants were analyzed per treatment per experiment. The effect of Benomyl on fungal ^{33}P translocation across the compartments was studied in low-P (100 μM P) MS agar in the absence of the plant by sampling a 1-cm^2 agar piece from the RHC 7 d after addition of ^{33}P to the HC (*SI Appendix*, Fig. S8*A*). For Benomyl-treated samples, the HC was covered with 1 mL of a Benomyl (Institute of Organic Industrial Chemistry, Warsaw) solution of 3 μg/mL (wt/vol), and plates were left open to dry for 1 h before addition of ^{33}P to the HC. The rest of the experiment was conducted as described above. The experiment was repeated three times with 5–20 replicates.

Phylogenetic Analysis of F229 and Related Ascomycetes. The F229 genome (NCBI BioProject PRJNA378526) was sequenced and annotated as described in *SI Appendix, Materials and Methods*. A multigene phylogenetic analysis was

conducted on 51 ascomycete genomes including F229. A phylogenetic tree was inferred from five housekeeping genes: 28S, 18S, Rpb1, Rpb2, and EF1α. For each gene, the nucleotide sequences retrieved from the genomes were aligned with MUSCLE (28), and informative positions were selected using Gblocks with relaxed parameters (52). Alignments were concatenated and used to compute a maximum-likelihood tree using PhyML (29) with the GTR+I+γ model and the SH-aLRT method for branch-support (1,000 iterations) calculation using Seaview (53).

Comparative Analysis of the Abundance of CAZymes in F229 and Related Ascomycetes. The abundance of CAZymes in the F229 genome was compared with that of 51 other ascomycetes genomes with plant-beneficial, plant-pathogenic, saprophytic, and plant unrelated lifestyles. In each genome, CAZyme modules were identified as described in *SI Appendix, Materials and Methods*, and their abundances were compared (Dataset S3). CAZyme profiles were compared by hierarchical clustering (Euclidean distances with average linkage method) in Morpheus (https://software.broadinstitute.org/morpheus/), and differences in the abundance of particular CAZymes between groups were assessed with *t* tests ($P < 0.01$).

Other experimental procedures are described in *SI Appendix, Materials and Methods*.

ACKNOWLEDGMENTS. We thank Janine Altmüller and Christian Becker at the Cologne Center for Genomics (https://portal.ccg.uni-koeln.de) for help with amplicon sequencing; the Max Planck Genome Center Cologne (mpgc.mpipz.mpg.de) for fungal genome sequencing; the Station Alpine Joseph Fourier (Jardin Botanique Alpin du Lautaret, https://www.jardinalpindulautaret.fr); Stefan Wötzel for plant cultivation; René Flisch (Agroscope Reckenholz) for providing soil; Nina Gerlach, Sabine Metzger, Stefanie Junkerman, and the Cologne Biocenter Mass Spectrometry Platform for ICP-MS analysis; and E. Kemen and A. Rondelet for valuable discussions and comments on the manuscript. This work was supported by funds from the Cluster of Excellence on Plant Sciences (J.A., M.B., G.J., A.Z., and G.C.); the Plant Fellows Programme (FP7 Marie Curie Actions, www.plantfellows.ch/; Grant GA-2010-267243 to J.A.); and the DFG Priority Program 1529 Adaptomics (J.W.).

1. Bulgarelli D, et al. (2012) Revealing structure and assembly cues for Arabidopsis root-inhabiting bacterial microbiota. *Nature* 488:91–95.
2. Berendsen RL, Pieterse CMJ, Bakker PAHM (2012) The rhizosphere microbiome and plant health. *Trends Plant Sci* 17:478–486.
3. Porras-Alfaro A, Bayman P (2011) Hidden fungi, emergent properties: Endophytes and microbiomes. *Annu Rev Phytopathol* 49:291–315.
4. Vandenkoornhuyse P, Quaiser A, Duhamel M, Le Van A, Dufresne A (2015) The importance of the microbiome of the plant holobiont. *New Phytol* 206:1196–1206.
5. Field KJ, Pressel S, Duckett JG, Rimington WR, Bidartondo MI (2015) Symbiotic options for the conquest of land. *Trends Ecol Evol* 30:477–486.
6. Smith SE, Read DJ (2010) *Mycorrhizal Symbiosis* (Academic, London).
7. Bucher M (2007) Functional biology of plant phosphate uptake at root and mycorrhiza interfaces. *New Phytol* 173:11–26.
8. Delaux P-M, et al. (2014) Comparative phylogenomics uncovers the impact of symbiotic associations on host genome evolution. *PLoS Genet* 10:e1004487.
9. Lambers H, et al. (2015) Phosphorus nutrition in Proteaceae and beyond. *Nat Plants* 1:15109.
10. van der Heijden MGA, Martin FM, Selosse M-A, Sanders IR (2015) Mycorrhizal ecology and evolution: The past, the present, and the future. *New Phytol* 205:1406–1423.
11. Richardson AE, Simpson RJ (2011) Soil microorganisms mediating phosphorus availability update on microbial phosphorus. *Plant Physiol* 156:989–996.
12. Hiruma K, et al. (2016) Root endophyte colletotrichum tofieldiae confers plant fitness benefits that are phosphate status dependent. *Cell* 165:464–474.
13. Bakshi M, et al. (2015) WRKY6 restricts Piriformospora indica-stimulated and phosphate-induced root development in Arabidopsis. *BMC Plant Biol* 15:305.
14. Yadav V, et al. (2010) A phosphate transporter from the root endophytic fungus Piriformospora indica plays a role in phosphate transport to the host plant. *J Biol Chem* 285:26532–26544.
15. Lundberg DS, et al. (2012) Defining the core Arabidopsis thaliana root microbiome. *Nature* 488:86–90.
16. Dombrowski N, et al. (2017) Root microbiota dynamics of perennial Arabis alpina are dependent on soil residence time but independent of flowering time. *ISME J* 11:43–55.
17. Wagner MR, et al. (2016) Host genotype and age shape the leaf and root microbiomes of a wild perennial plant. *Nat Commun* 7:12151.
18. Shakya M, et al. (2013) A multifactor analysis of fungal and bacterial community structure in the root microbiome of mature Populus deltoides trees. *PLoS One* 8:e76382.
19. de Souza RSC, et al. (2016) Unlocking the bacterial and fungal communities assemblages of sugarcane microbiome. *Sci Rep* 6:28774.
20. Coleman-Derr D, et al. (2016) Plant compartment and biogeography affect microbiome composition in cultivated and native Agave species. *New Phytol* 209:798–811.
21. Kohler A, et al.; Mycorrhizal Genomics Initiative Consortium (2015) Convergent losses of decay mechanisms and rapid turnover of symbiosis genes in mycorrhizal mutualists. *Nat Genet* 47:410–415.
22. Peter M, et al. (2016) Ectomycorrhizal ecology is imprinted in the genome of the dominant symbiotic fungus Cenococcum geophilum. *Nat Commun* 7:12662.
23. Fesel PH, Zuccaro A (2016) Dissecting endophytic lifestyle along the parasitism/mutualism continuum in Arabidopsis. *Curr Opin Microbiol* 32:103–112.
24. Törüng P, et al. (2015) Large-scale adaptive differentiation in the alpine perennial herb Arabis alpina. *New Phytol* 206:459–470.
25. Willing E-M, et al. (2015) Genome expansion of Arabis alpina linked with retrotransposition and reduced symmetric DNA methylation. *Nat Plants* 1:14023.
26. Edwards J, et al. (2015) Structure, variation, and assembly of the root-associated microbiomes of rice. *Proc Natl Acad Sci USA* 112:E911–E920.
27. Peiffer JA, et al. (2013) Diversity and heritability of the maize rhizosphere microbiome under field conditions. *Proc Natl Acad Sci USA* 110:6548–6553.
28. Edgar RC (2004) MUSCLE: Multiple sequence alignment with high accuracy and high throughput. *Nucleic Acids Res* 32:1792–1797.
29. Guindon S, et al. (2010) New algorithms and methods to estimate maximum-likelihood phylogenies: Assessing the performance of PhyML 3.0. *Syst Biol* 59:307–321.
30. Glynou K, et al. (2016) The local environment determines the assembly of root endophytic fungi at a continental scale. *Environ Microbiol* 18:2418–2434.
31. Larsen J, Thingstrup I, Jakobsen I, Rosendahl S (1996) Benomyl inhibits phosphorus transport but not fungal alkaline phosphatase activity in a Glomus–cucumber symbiosis. *New Phytol* 132:127–133.
32. Persson BL, et al. (1998) Phosphate permeases of Saccharomyces cerevisiae. *Biochim Biophys Acta* 1365:23–30.
33. Tedersoo L, et al. (2014) Fungal biogeography. Global diversity and geography of soil fungi. *Science* 346:1256688.
34. Talbot JM, et al. (2014) Endemism and functional convergence across the North American soil mycobiome. *Proc Natl Acad Sci USA* 111:6341–6346.
35. Peay KG, Kennedy PG, Talbot JM (2016) Dimensions of biodiversity in the Earth mycobiome. *Nat Rev Microbiol* 14:434–447.
36. Peay KG, Bidartondo MI, Arnold AE (2010) Not every fungus is everywhere: Scaling to the biogeography of fungal-plant interactions across roots, shoots and ecosystems. *New Phytol* 185:878–882.
37. Willmann M, et al. (2013) Mycorrhizal phosphate uptake pathway in maize: Vital for growth and cob development on nutrient poor agricultural and greenhouse soils. *Front Plant Sci* 4:533.
38. Alcázar R, Parker JE (2011) The impact of temperature on balancing immune responsiveness and growth in Arabidopsis. *Trends Plant Sci* 16:666–675.
39. Toju H, Tanabe AS, Ishii HS (2016) Ericaceous plant-fungus network in a harsh alpine-subalpine environment. *Mol Ecol* 25:3242–3257.
40. Tedersoo L, et al. (2009) Ascomycetes associated with ectomycorrhizas: Molecular diversity and ecology with particular reference to the Helotiales. *Environ Microbiol* 11:3166–3178.
41. Smith SE, Smith FA, Jakobsen I (2003) Mycorrhizal fungi can dominate phosphate supply to plants irrespective of growth responses. *Plant Physiol* 133:16–20.
42. Bougoure J, et al. (2014) High-resolution secondary ion mass spectrometry analysis of carbon dynamics in mycorrhizas formed by an obligately myco-heterotrophic orchid: Rhizanthella nanoSIMS analysis. *Plant Cell Environ* 37:1223–1230.
43. Usuki F, Narisawa K (2007) A mutualistic symbiosis between a dark septate endophytic fungus, Heteroconium chaetospira, and a nonmycorrhizal plant, Chinese cabbage. *Mycologia* 99:175–184.
44. Behie SW, Zelisko PM, Bidochka MJ (2012) Endophytic insect-parasitic fungi translocate nitrogen directly from insects to plants. *Science* 336:1576–1577.
45. Lahrmann U, et al. (2015) Mutualistic root endophytism is not associated with the reduction of saprotrophic traits and requires a noncompromised plant innate immunity. *New Phytol* 207:841–857.
46. Kubicek CP, Starr TL, Glass NL (2014) Plant cell wall-degrading enzymes and their secretion in plant-pathogenic fungi. *Annu Rev Phytopathol* 52:427–451.
47. Hacquard S, et al. (2016) Survival trade-offs in plant roots during colonization by closely related beneficial and pathogenic fungi. *Nat Commun* 7:13072.
48. Schloss PD, et al. (2009) Introducing mothur: Open-source, platform-independent, community-supported software for describing and comparing microbial communities. *Appl Environ Microbiol* 75:7537–7541.
49. Oksanen J, Blanchet G, Kindt R (2016) Vegan: Community Ecology Package. Available at cran.r-project.org/package=vegan.
50. Dray S, Dufour A-B (2007) The ade4 package: Implementing the duality diagram for ecologists. *J Stat Softw* 22:1–20.
51. van der Ent A, Baker AJM, Reeves RD, Pollard AJ, Schat H (2013) Hyperaccumulators of metal and metalloid trace elements: Facts and fiction. *Plant Soil* 362:319–334.
52. Castresana J (2000) Selection of conserved blocks from multiple alignments for their use in phylogenetic analysis. *Mol Biol Evol* 17:540–552.
53. Gouy M, Guindon S, Gascuel O (2010) SeaView version 4: A multiplatform graphical user interface for sequence alignment and phylogenetic tree building. *Mol Biol Evol* 27:221–224.

SI Appendix

Materials and Methods

A. alpina accessions, plant growing locations and soils used

The experimental set-up is shown in Figure 1 A. *A. alpina* accession Pajares (PM) was collected in Spain (1). *A. alpina* accessions E3, S2, F1gal originate from natural *A. alpina* populations located in Spain (E3), Sweden (S2) (2) and France (F1gal) (3) (Table S1). Except for PM, seeds were harvested from the natural population. Seeds are available from Jörg Wunder or George Coupland (Department of Plant Developmental Biology, Max Planck Institute for Plant Breeding Research, Cologne, Germany). In the alpine common garden experiment ('GAR') these four accessions were grown side by side in the Lautaret garden (France). In the same common garden plot, soil 'Lau' was harvested in September 2013 for the greenhouse experiment. The other two soils 'RecNK' and 'RecNPK' used in the greenhouse ('GrH') experiment were harvested in two agricultural fields that have been fertilized with N (Nitrogen) and K (Potassium) fertilizer with (RecNPK) and without P (RecNK) for 24 years at the Research Station Agroscope Reckenholz-Tänikon (ART) (Switzerland). Wild-growing *A. alpina* plants were harvested near the Lautaret common garden at the natural site 'Col du Galibier' (France) (3) in two consecutive years (July 2013 and October 2014). Soil 'Gal' was sampled at the same location in Sepember 2013 for microcosm experiments. For all the soils, the top layer (0 - 10 cm) was removed and the soil was harvested from a depth of 10 - 30 cm. All the soils were dried for 3 - 4 days at ambient temperature, mixed and sieved at 1 cm grain size before storing them at 4 °C until further use. Soil characteristics are given in Table S2.

Greenhouse experiment ('GrH')

In the greenhouse experiment *A. alpina* PM was grown on soils 'RecNK', 'RecNPK' and 'Lau' for three months. Seeds from *A. alpina* PM were surface sterilized by shaking for 15 min in 70 % ethanol with 0.01 % Triton X-100, followed by a final wash in 100 % ethanol. Seeds were stratified for 1 week at 4 °C before sowing 4 seeds in 1 L pots containing 1 kg of soil. Plants were grown for three months in the greenhouse at 22 °C with additional illumination (16h/8h day/night cycle). At the beginning of the experiment soil humidity and water-holding capacity were measured and soil humidity was maintained at ~ 70 % of the water-holding capacity by weighing and watering the pots every other day. Three unplanted (bulk soil sampling) and six planted pots per soil type were prepared. All the plants from a pot (1 - 4 plants) were pooled into one sample for shoot, root and rhizosphere sampling (n = 6).

Common garden experiment ('GAR')

In the alpine common garden experiment different *A. alpina* accessions were grown on soil 'Lau' for three months. Non-surface sterilized seeds from *A. alpina* accessions PM, E3, S2 and F1gal were stratified for 4 days at 4°C before sowing in peat-based soil for germination. Plants were grown under greenhouse conditions (22 °C with additional lightning 16h/8h day/night cycle, at the Max Planck Institute for Plant Breeding Research, Cologne, Germany) for 4 weeks before transplanting them to the plot in the Lautaret garden (France) in June 2013. In September 2013, after 3 months of growth, 5 to 6 randomly chosen plants per accession (including the surrounding soil) were put in individual 5 L pots and brought to the Botanical Institute of University of Cologne for shoot, root endosphere and rhizosphere sampling from individual plants (n = 5 to 6). Unplanted soil was harvested (1 Kg) and used for the collection of bulk soil samples (n = 3).

Plant harvesting from a natural alpine population ('WILD')

Wild-growing *A. alpina* plants were harvested in an area of approx. 20 m^2 from a natural population at the Col du Galibier (French Alps, coordinates N45°3'38.592"/E6°24'8.784", 2640 m above sea level) in July 2013 and September 2014. Five randomly-chosen plants and 1 kg of unplanted soil were collected as described above and brought to the Botanical Institute for shoot, root endosphere and rhizosphere sampling from individual plants (n = 5 to 6) and for bulk soil sampling from unplanted soil (n = 3).

Root, rhizosphere, bulk soil sampling and DNA extraction

The sampling was conducted as described by Bulgarelli et al. (2012) (4). Briefly, plants were dug out of the soil, roots were shaken to detach loosely adhering soil, and root sections, with tightly adhering rhizosphere soil, were collected from the zone spanning 3 to 7 cm below the stem and washed in 15 ml tubes filled with 5 ml of Silwet washing solution (130 mM NaCl, 7 mM Na_2HPO_4, 3 mM NaH_2PO_4, pH 7.0, 0.02% Silwet L-77) for 20 min at 180 rpm. After repeating the washing step, roots were transferred to a new 15 ml tube containing 5 ml of Silwet washing solution and were sonicated (10 cycles, each for 30 s at 160 W followed by a 30 s pause) in a Bioruptor (Bioruptor Next Gen UCD-300, Diagenode, Liège, Belgium). Roots were then blot dried on filter paper, frozen in liquid nitrogen and stored at -80°C. To recover the rhizosphere soil, the first washing solution was centrifuged (20 min at 1500 *g*) and the pellet was frozen in liquid nitrogen and stored at - 80°C. For bulk soil sampling soil was recovered from the center of unplanted pots (greenhouse experiment) or unplanted area (common garden experiment and natural site) at a depth of 3 to 7 cm. Genomic DNA (gDNA) was extracted from root, rhizosphere soil and bulk soil samples using the FastDNA SPIN Kit for Soil (MP Biomedicals, Solon, USA) and quantified with a Nanodrop spectrophotometer (PeqLab Biotechnology, Erlangen, Germany). Two "blank" DNA

extractions with no sample added were included in the sequencing run to serve as controls for kit related DNA contamination (Fig. S13 B).

Fungal ITS2 sequencing

Fungal community description was carried out by sequencing the ITS2 region of the fungal rRNA operon, which serves as a fungal taxonomical marker. In a preliminary study the three forward primers described by Ihrmarck et al. (2012) (5) (ITS9, fITS7 and gITS7) were tested in combination with reverse primer ITS4 (6), on three root and three rhizosphere samples from *A. alpina* (Fig. S1). ITS2 PCR amplification included reverse primer ITS4 at 300 nM and one of the three forward primers ITS9 (1000 nM), fITS7 (500 nM) or gITS7 (500 nM). Annealing temperatures were 55, 57, and 56°C for ITS4/ITS9, ITS4/fITS7 and ITS4/gITS7, respectively. In order to have comparable amounts of PCR product, the number of cycles in the first PCR was adjusted to 30, 26 and 25 for ITS4/ITS9, ITS4/fITS7 and ITS4/gITS7, respectively. For multiplexing, both forward and reverse primers were tagged with twelve tag sets described in Gloor et al. (2010) (7) by adding 4 to 7 bases to the 5' end (see Table S4 for primer and tag information). To reduce primer tag-dependent PCR bias (8) we used a two-step PCR method. The first PCR was conducted with non-tagged primers in 25 µl reactions containing 0.1 U/µl GoTaq G2 Flexi DNA polymerase (Promega, Mannheim, Germany), 1x Green GoTaq Flexi Buffer (Promega), 0.2 mM dNTPs, 2.75 mM $MgCl_2$, and 20 ng of gDNA. PCR cycling conditions were 95°C for 5 min followed by 25 to 30 amplification cycles (95°C x 30 sec, 55 to 57°C x 30 sec, 72°C x 30 sec), followed by a final elongation at 72°C during 7 min. The first PCR samples were diluted 1:5 with water and 5 µl were subsequently used in the second PCR conducted with tagged primers. PCR conditions were the same as for the first PCR except that amplification was limited to 5 cycles. PCRs were conducted on a Veriti Thermal Cycler (Applied Biosystems, Carlsbad, CA,

USA). A negative water control sample was included in each PCR run for each PCR master mix. PCR reactions were subjected to gel electrophoresis in agarose (1.5 % w/v) to verify DNA amplification and check the negative controls. Four PCR reactions per sample were pooled, purified with a NucleoSpin PCR Clean-Up Kit (Macherey-Nagel, Düren, Germany) and DNA was quantified with a Nanodrop spectrophotometer (PeqLab). Twelve randomly chosen amplicon samples with different tag sets were pooled in equimolar amounts into one library. Library preparation and indexing was done with the MiSeq Reagent Kit v3 for 2 x 300 base paired-end sequencing (Illumina, San Diego, CA, USA). All the samples in the preliminary study were run in a single MiSeq run with 3% Phix control at the Cologne Center for Genomics (University of Cologne, Cologne, Germany).

In the final study, primer set ITS4/ITS9 was selected based on the observations that it generated a higher percentage of fungal ITS2 sequences (Fig. S1 B) and recovered a higher number of low abundance fungal orders (< 0.5 % relative abundance; Fig. S1 C) probably due to its lower affinity to *A. alpina* ITS2 (Fig. S1 A). ITS2 amplification and sequencing were conducted as described above. When the PCR failed to produce sufficient DNA product, it was repeated using less gDNA (10 ng) and five more (35) amplification cycles in the first PCR. Two 'PCR water control' samples were included in the final sequencing run to account for environmental DNA contamination during PCR (Fig. S13 B). In the final sequencing run environmental DNA contamination accounted for only 20 - 40 reads in the 'PCR water control' and 'blank DNA extraction' controls. Seed derived fungal contamination was also low and accounted to a maximum of 87 fungal reads (in 20 pooled seedlings) given that most of the reads corresponded to *A. alpina* ITS2 sequences (Fig. S13 B).

Sequencing data analysis

Sequencing data was analyzed in Mothur v.1.37.3 (9). Paired-end (PE) forward and reverse reads were assembled into contigs using the *make.contigs* command, and only PE reads with at least five bases overlap (full match) between the forward and reverse reads were selected using the *screen.seqs* command. PE reads were demultiplexed, filtered to maximum two mismatches with the primer-tag sequence and a minimum of 100 bases in length, and the primer-tag sequences were trimmed (*trim.seqs* command). Reads differing by less than three bases were clustered together (*pre.cluster* command) and chimeras were filtered using Uchime in Mothur (*chimera.uchime* command) with abundant sequences as reference. Sequences were clustered into operational taxonomical units (OTU) at the 97 % similarity threshold using VSEARCH in Mothur with the abundance greedy clustering method (agc) (*cluster* command). Individual sequences were taxonomically classified using the rdp classifier (confidence threshold set to 60) and the UNITE fungal ITS database (10) (UNITE+INSD release 31.01.2016). *Arabis alpina* ITS2 sequences were manually included in the database using the *classify.seqs* command. Each OTU was taxonomically classified (*classify.otu* command with confidence threshold set to 60), plant OTUs and OTUs with unknown taxonomy at the kingdom level were deleted, and low abundance OTUs were also removed (< 50 reads) using the *split.abund* command. Rarefaction curves were produced for each sample (*rarefaction.single* command) by re-sampling 100 reads without replacement for 1000 iterations (Fig. S13 A). The sequencing summary is given in Table S5. The relative abundance of each OTU in each sample was calculated from the final OTU table. The most abundant sequence within each OTU was selected as the ITS2 sequence representative for this given OTU.

Isolation of root fungal endophytes and identification by ITS sequencing

For the isolation and culture of fungal endophytes, *A. alpina* root samples were collected in the different treatments and experiments. Roots were washed twice in sterile water before surface sterilization (1 min in 70 % ethanol, 4 min in 3 % NaClO, 30 s in 70 % ethanol and 3 washes in water for 1 min). Roots were then cut into 1 - 2 cm pieces, sonicated in a Bioruptor (10 cycles, of 30 s at 160 W and 30 s pause) and plated individually onto MYP agar (1L contained 7 g malt extract, 1 g tryptone-peptone casein, 0.5 g yeast extract, 12 g agar), PDA agar (US Biological Life sciences, Salem, MA, USA) or minimal medium agar (1L contained 15 g glucose, 2 g NH_4NO_3, 0.5 g KCl, 0.5 g $MgSO_4.7H_2O$, 0.3 g $MnSO_4.4H_2O$, 0.3 g $FeSO_4.7H2O$, 15 g Agar, pH adjusted to 5.5). Plates were checked regularly for four weeks and growing fungi were directly replicated onto new plates. Fungal growth was observed in 10 % of the plated root pieces. DNA was extracted from agar colonies by grinding 300 mg mycelium in 400 µl of extraction buffer (200 mM Tris-Hcl pH 7.5, 250 mM NaCl, 25 mM EDTA and 0.5 % SDS) followed by centrifugation (11 000 *g* X 5 min). The supernatant was recovered and nucleic acids were precipitated for 2 min at room temperature using 1 volume of isopropanol followed by centrifugation (11 000 *g* X 10 min). The pellet was washed once with 70% ethanol and resuspended in sterile water. The gDNA was used for full-length ITS PCR amplification and sequencing for fungal identification. PCR reaction mixtures were the same as for ITS2 amplification except that primers were replaced with primers ITS4 (11) and ITS1 (6) or ITS4 and ITS5 (11) at 100 nM. PCR cycling conditions were 95°C x 5 min followed by 35 amplification cycles (95°C x 45 sec, 52°C x 30 sec, 72°C x 90 sec) and a final elongation at 72°C x 7min. ITS amplicons were sequenced by Sanger technology (GATC Biotech, Konstanz, Germany). Agar plugs of fungal isolates were kept in water at 4°C or in 10 % glycerol at - 80 °C for long term storage. The fungal isolates were taxonomically classified based on their full ITS sequence using Mothur and the UNITE database as described before. Their ITS2 sequences were classified within the described OTUs (established from ITS2 sequencing) based on an ITS2 sequence identity of ≥ 97 % relative to the representative OTU sequence. Recovered isolates were deposited in our Cologne Collection of Root-Associated Fungi (CORFU) and are

listed in a supplementary file (Dataset S1). From the 136 fungal isolates recovered from surface sterilized *A. alpina* roots, 132 could be classified within 36 of the 1917 fungal OTUs detected in *A. alpina* roots by ITS2 sequencing. This indicated that the collection represents 1.87 % of the fungal root OTUs. When the 100 most prevailing OTUs detected were considered (detected in ≥ 46 % of the samples) this proportion increased to 19 %.

Impact of fungal inoculation on A. alpina growth on MS agar

Fungus 229 (F229) as well as other fungal isolates (isolates 226, 248, 247, 91, 83 and 222) were screened for their effect on root and shoot growth of *A. alpina* F1gal and PM under high and low P conditions. *A. alpina* F1gal and PM seeds were surface sterilized as described above, plated onto low-P MS agar (100 µM P as KH_2PO_4) (12), stratified one week at 4°C and let to germinate in a phytochamber (Versatile Environmental Test Chamber, Sanyo, Osaka, Japan; 16h/8h day/night cycles at 22/18°C and 70% relative humidity). One-week-old seedlings were then transferred to new plates containing 40 ml of low-P (100 µM P as KH_2PO_4) or high-P (1000 µM P as KH_2PO_4) MS medium, respectively. Two weeks old fungal MYP agar plates were used to inoculate low-P MS agar plates by transferring a 0.5 cm^3 agar plug. The fungus was let to grow on low-P MS agar for two weeks prior to inoculating one week-old seedlings by placing a 1 mm^3 agar plug 0.5 cm under the root tip. Plugs from fungus-free low-P MS plates were used for mock-inoculated plants. Plates were closed with Micropore Surgical Tape (3M, Borken, Germany), placed vertically in the phytochamber and plants were let to grow for two weeks under the same conditions as indicated above. The plates were randomized every other day. After two weeks (14 dpi) plants were harvested individually, shoot weight was measured and individual root systems were washed and scanned in a transparent tray filled with water using a backlit scanner (Perfection V700, Epson, Meerbusch, Germany). Grey scale images were analyzed with

WinRHIZO software (Regent Instruments, Quebec, Canada) to estimate total root length and total root surface area. Each fungus was tested once in four experiments including different fungi (Fig. S4 B).

The effect of isolate 229 (OTU00005) on *A. alpina* F1gal growth under low- and high-P MS agar conditions, was further assessed in three independent experiments each including four plates per treatment and four plants per plate (n = 16). The experiments were performed as indicated above except that all the shoots from one plate were pooled to measure shoot P content by ICP-MS and one root system per plate was collected for microscopy analysis of fungal colonization. The positive effect of a second isolate belonging to OTU00005 (isolate 240) on *A. alpina* F1gal root growth under low P conditions was assessed (as described above) in three independent experiments each including five plates per treatment and four plants per plate (n = 20). Data normality was checked and means were compared with *t*-test ($P < 0.05$).

Microscopy analysis

For microscopy analysis of fungal colonization, fungal and plant cell walls were stained with WGA-Alexa 488 (Molecular Probes, Eugene, OR, USA) and propidium iodide, respectively. Root samples were kept in 50% ethanol before clearing in 20 % KOH for 30 min at 100 °C. After rinsing in deionized water roots were acidified in 0.1 M HCl for 2 h. Roots were then placed in a staining solution of PBS buffer with 10 µg/ml of propidium iodide and 5 µg/ml of WGA-Alexa Fluor 488 and were infiltrated for 6 min with a vacuum pump (Concentrator plus, Eppendorf, Hamburg, Germany). Samples were mounted on glass slides in 10 % glycerol for microscopy analysis. For vital staining with FM 4-64, fresh plant roots were washed twice in PBS buffer before infiltration for 2 x 4 min with PBS staining solution containing 5 µg/ml of WGA-Alexa Fluor 488 and 2 µg/ml of FM 4-64FX (Molecular Probes). Samples were mounted in water and observed directly.

Microscopy analyses were conducted with a SP8 CLSM microscope (Leica, Mannheim, Germany) with excitation and detection parameters set to 561 nm and 570 - 700 nM for propidium iodide, 488 nm and 500 - 600 nM for WGA-Alexa Fluor 488 and 561 nm and 650 - 750 nM for FM 4-64. Fungal colonization of roots was quantified under a fluorescence microscope (DM5000, Leica) by taking 60 images (740 × 985 µm) per root sample (with three root samples per treatment). The number of hyphae per image were estimated using the intersection method often used for the calculation of root colonization by arbuscular mycorrhizal fungi (13), and for each image fungal colonization was scored as no colonization (no hyphae), colonization low (1 - 50 hyphae) or colonization high (>50 hyphae). The colonization level was calculated as the percentage of images where at least one hyphae was recorded divided by the total number analyzed images. The colonization patterns (i.e. the number of fields with no, low or high colonization) were then compared between low P and high P conditions, with a chi-squared test ($P < 0.05$).

Fungus 229 genome and transcriptome sequencing

For genome sequencing, high molecular weight gDNA was extracted and used for PacBio SMRT technology sequencing. Fungus 229 was grown for three weeks on MYP agar, the mycelium was scraped from the surface of four plates and was ground in liquid nitrogen. Genomic DNA was extracted by adding 1 ml of extraction buffer (100 mM Tris-HCL, 1.5 M NaCl, 50 mM EDTA, 2 % CTAB, 0.05 % β-mercaptoethanol) to 200 mg of mycelium, shaking for 10 min at room temperature, adding 1 ml CIA (chloroform:isoamylalcohol 24:1), shaking for 5 min, centrifuging (20 min at 10000 *g*) and recovering the supernatant. The solution was cleared by adding 0.2 volumes of ethanol to the supernatant, shaking for 5 min, adding 1 volume of CIA, centrifuging (20 min at 10000 *g*) and recovering the supernatant. DNA was precipitated by addition of 1 volume

of isopropanol to the supernatant, shaking for 1 h at room temperature and centrifuging (20 min at 5000 *g*). The pellet was washed with 70 % ethanol, dried and resuspended in 10 mM Tris-HCl, pH 8.5. DNA was further cleaned-up following the Pacific Biosciences (Menlo Park, CA, USA) protocol using a salt:chloroform wash (available at http://www.pacb.com/wp-content/uploads/2015/09/Shared-Protocol-Guidelines-for-Using-a-Salt-Chloroform-Wash-to-Clean-Up-gDNA.pdf). The genome sequence of F229 was generated using PacBio RS II technology (Pacific Biosciences). Large SMRTbell gDNA libraries with insert size of 15 kb were prepared and 9 SMRT cells were sequenced at the Max Planck-Genome-center Cologne. The PacBio reads were further assembled into 39 contigs by Overlap-Layout-Consensus algorithm using HGAP with SMRT Analysis Software v2.3.0 (Pacific Biosciences). The genome was deposited at the NCBI data base (BioProject PRJNA378526) under the name “Helotiales sp. F229” genome assembly and annotation information is given in the Dataset S2.

The transcriptome of F229 growing on MYP media was included in the analysis to aid in gene annotation. The fungus was grown for one week on MYP agar, the mycelium was scraped from the agar surface and RNA was extracted using a NucleoSpin RNA Plant kit (Macherey Nagel). The RNA sample was used for polyA-selected library preparation using a TruSeq RNA kit (Illumina) and paired-end sequencing (2 × 75b) in a Hiseq instrument (Illumina) at the Cologne Center for Genomics (http://portal.ccg.uni-koeln.de/ccg/index.php). Reads were trimmed to remove unidentified and low-quality bases and reads with less than 50 bp were discarded. All the paired and unpaired reads were then assembled using Trinity v.2.1.1 (14) into transcripts (including alternative spliced variants) and genes. These *de novo*-assembled transcripts were then used for gene prediction.

Gene prediction

The Maker (15), Braker (16), SNAP (17) and Augustus (18) pipelines were used together with the *de novo* assembled transcripts as EST hints, and the protein sequences of the closely related fungus *Marssonina brunnea f. sp. multigermtubi MB_m1* (DOE Jpint Genome Institute id Marbr1), to predict the genes from the assembled genome. Maker pipeline with Augustus prediction resulted in 12.059 transcripts (with alternative splicing variants) whereas Maker with SNAP and Augustus predictions generated 12.893 transcripts. Braker predicted 17.471 transcripts and 16.962 genes by using RNA-seq reads aligned against the assembled genome. To compare the completeness of the three predicted gene-sets, we screened them for the 1.438 single copy orthologs common to most fungi (> 90 %) identified in the BUSCO gene set (Benchmarking Universal Single-Copy Orthologs, v1.22, (19)). In the gene-sets obtained from Maker (with and without SNAP) only 93.5 % of the BUSCO orthologs were found, while 99.4 % of them were found in the Braker gene-set. Hence the gene-set from Braker was selected for further analysis. The completeness of the final gene set was additionally assessed by searching for the 246 conserved fungal genes in the FUNYBASE database (20) and the 248 core eukaryotic genes in CEG database (21) (BLASTX, E-value < 10^{-5}) and 98.7 % and 99.2 % of those genes were found, respectively.

Gene annotation

To annotate the predicted genes a BLASTX search against the non-redundant protein NCBI database was performed (E-value < 10^{-5}, maximum hits = 20). Gene ontology analysis was carried out using BLAST2GO (22). KEGG annotation for the 16.962 predicted proteins, was carried out using using GhostKOALA (23) resulting in 4.057 (23.9 %) proteins which were assigned to KO identifiers and mapped against the KEGG database using KEGG Mapper to identify pathways. Pathogenicity related proteins were searched against PHI database using BLASTP (E-value < 10^{-}

289 ^{5}). To predict tRNA genes, the assembled genome was scanned with tRNAscan-SE (v.1.3.1, (24))
290 using “Cove only” mode and the eukaryotic gene model. RNAmmer (v.1.2, (25)) was used with
291 eukaryotic mode to predict the 18S, 28S and 8S ribosomal RNAs.

292

293 Protein family analysis

294 Protein family analysis (Pfam analysis, (26)) was done by searching the protein sequences in the
295 Pfam database (E-value < 10^{-5}). dbCAN (27) was used to predict genes with domains of
296 Carbohydrate-Active Enzymes (CAZymes, (28)). The number of domains of CAZyme classes
297 including glycoside hydrolases (GH), glycosyltransferases (GT), carbohydrate-binding modules
298 (CBM), carbohydrate esterases (CE), polysaccharide lyases (PL) and proteins with auxiliary
299 activities (AA) was determined and the number of genes encoding the respective domains were
300 examined. From the 900 genes containing CAZyme domains 349 contained a GH domain, 160
301 contained a CE domain, 135 contained a AA domain, 122 contained a GT domain, 109 contained
302 a CBM domain and 23 contained a PL domain.

303

304 Repetitive elements

305 The assembled genomic contigs were scanned for repetitive elements using RepeatMasker
306 v.4.0.6 (29) run with rmblast v2.2.23+ and the fungi repeat library from RepBase (30)
307 (http://www.giriinst.org/repbase/index.html, RepeatMasker repeat database v.20150807). Simple
308 Sequence Repeats (SSR) in the genome were identified with MISA (31) using standard settings
309 for SSR with minimum length of 10 bp and repeat length of mono-10, di-6, tri-5, tetra-5, penta-5
310 and hexa-5 (Dataset S2).

311

Secretome prediction

SignalP v.4.0 (32) and TargetP (package v.1.1, (33)) were used to predict the proteins with a signal peptide, which were further assessed with TMHMM (v2.0, (34)) for presence of a transmembrane domain. The proteins with a transmembrane domain not overlapping the signal peptide were discarded to remove non-secreted proteins. From the predicted secretome comprising 1315 proteins, 604 proteins with size ≤300 aa were selected as putative effector candidates, as described in Lahrmann et al. (2015) (35).

Phylogenetic analysis of P transporters in F229 genome

Protein sequences from annotated P transporters (PTs) in F229 genome were phylogenetically compared to described PTs in Saccharomyces cerevisiae (ScPHO84, KZV08715; ScPHO87, KZV12886; ScPHO88, CAA85061; ScPHO89, KZV13384; ScPHO90, KZV10076; ScPHO91, DAA10554) and to fungal PTs known to be involved in fungus to plant P transfer in AM fungi *Glomus versiforme* (GvPT, Accession number AAC49132), *Rhizophagus intraradices* (GiPT, AAL37552) and *Funneliformis mosseae*, (GmosPT, AAZ22389); the EM fungus *Hebeloma cylindrosporum* (HcPT2, CAI94747); and the endophytic fungus *Serendipita indica* (PiPT, ABI93950). Protein sequences were aligned using muscle and the was conducted phylogenetic reconstruction using Phy-ML (LG model) under Seaview with 100 bootstrap replicates. PT sequences from F229 genome are given in the Dataset S2.

References

1. Wang R, et al. (2009) PEP1 regulates perennial flowering in Arabis alpina. *Nature* 459(7245):423–427.

2. Toräng P, et al. (2015) Large-scale adaptive differentiation in the alpine perennial herb Arabis alpina. *New Phytol* 206(1):459–470.

3. Dombrowski N, et al. (2017) Root microbiota dynamics of perennial Arabis alpina are dependent on soil residence time but independent of flowering time. *ISME J* 11(1):43–55.

4. Bulgarelli D, et al. (2012) Revealing structure and assembly cues for Arabidopsis root-inhabiting bacterial microbiota. *Nature* 488(7409):91–95.

5. Ihrmark K, et al. (2012) New primers to amplify the fungal ITS2 region – evaluation by 454-sequencing of artificial and natural communities. *FEMS Microbiol Ecol* 82(3):666–677.

6. Gardes M, Bruns TD (1993) ITS primers with enhanced specificity for basidiomycetes - application to the identification of mycorrhizae and rusts. *Mol Ecol* 2(2):113–118.

7. Gloor GB, et al. (2010) Microbiome Profiling by Illumina Sequencing of Combinatorial Sequence-Tagged PCR Products. *PLOS ONE* 5(10):e15406.

8. Berry D, Mahfoudh KB, Wagner M, Loy A (2011) Barcoded Primers Used in Multiplex Amplicon Pyrosequencing Bias Amplification. *Appl Environ Microbiol* 77(21):7846–7849.

9. Schloss PD, et al. (2009) Introducing mothur: Open-Source, Platform-Independent, Community-Supported Software for Describing and Comparing Microbial Communities. *Appl Environ Microbiol* 75(23):7537–7541.

10. Kõljalg U, et al. (2013) Towards a unified paradigm for sequence-based identification of fungi. *Mol Ecol* 22(21):5271–5277.

11. White T., Bruns T, Lee S (1990) Amplification and direct sequencing of fungal ribosomal RNA genes for phylogenetics. *PCR Protocols: A Guide to Methods and Applications* (Academic Press, Inc., New York.), pp 315–322.

12. Murashige T, Skoog F (1962) A Revised Medium for Rapid Growth and Bio Assays with Tobacco Tissue Cultures. *Physiol Plant* 15(3):473–497.

13. McGONIGLE TP, Miller MH, Evans DG, Fairchild GL, Swan JA (1990) A new method which gives an objective measure of colonization of roots by vesicular—arbuscular mycorrhizal fungi. *New Phytol* 115(3):495–501.

14. Grabherr MG, et al. (2011) Full-length transcriptome assembly from RNA-Seq data without a reference genome. *Nat Biotechnol* 29(7):644–52.

15. Campbell MS, Holt C, Moore B, Yandell M (2014) Genome Annotation and Curation Using MAKER and MAKER-P. *Curr Protoc Bioinforma* 48:4.11.1-39.

16. Hoff KJ, Lange S, Lomsadze A, Borodovsky M, Stanke M (2016) BRAKER1: Unsupervised RNA-Seq-Based Genome Annotation with GeneMark-ET and AUGUSTUS. *Bioinformatics* 32(5):767–9.

17. Korf I (2004) Gene finding in novel genomes. *BMC Bioinformatics* 5:59.

18. Stanke M, et al. (2006) AUGUSTUS: ab initio prediction of alternative transcripts. *Nucleic Acids Res* 34(Web Server issue):W435-9.

19. Simão FA, Waterhouse RM, Ioannidis P, Kriventseva EV, Zdobnov EM (2015) BUSCO: assessing genome assembly and annotation completeness with single-copy orthologs. *Bioinformatics* 31(19):3210–2.

20. Marthey S, et al. (2008) FUNYBASE: a FUNgal phYlogenomic dataBASE. *BMC Bioinformatics* 9:456.

21. Parra G, Bradnam K, Korf I (2007) CEGMA: a pipeline to accurately annotate core genes in eukaryotic genomes. *Bioinformatics* 23(9):1061–7.

22. Conesa A, et al. (2005) Blast2GO: a universal tool for annotation, visualization and analysis in functional genomics research. *Bioinformatics* 21(18):3674–6.

23. Kanehisa M, Sato Y, Morishima K (2016) BlastKOALA and GhostKOALA: KEGG Tools for Functional Characterization of Genome and Metagenome Sequences. *J Mol Biol* 428(4):726–31.

24. Lowe TM, Eddy SR (1997) tRNAscan-SE: a program for improved detection of transfer RNA genes in genomic sequence. *Nucleic Acids Res* 25(5):955–64.

25. Lagesen K, et al. (2007) RNAmmer: consistent and rapid annotation of ribosomal RNA genes. *Nucleic Acids Res* 35(9):3100–8.

26. Finn RD, et al. (2014) Pfam: the protein families database. *Nucleic Acids Res* 42(Database issue):D222-30.

27. Yin Y, et al. (2012) dbCAN: a web resource for automated carbohydrate-active enzyme annotation. *Nucleic Acids Res* 40(Web Server issue):W445-51.

28. Lombard V, Golaconda Ramulu H, Drula E, Coutinho PM, Henrissat B (2014) The carbohydrate-active enzymes database (CAZy) in 2013. *Nucleic Acids Res* 42(Database issue):D490-5.

29. Chen N (2004) Using RepeatMasker to identify repetitive elements in genomic sequences. *Curr Protoc Bioinforma* Chapter 4:Unit 4.10.

30. Jurka J, et al. (2005) Repbase Update, a database of eukaryotic repetitive elements. *Cytogenet Genome Res* 110(1–4):462–7.

31. Thiel T, Michalek W, Varshney R, Graner A (2003) Exploiting EST databases for the development and characterization of gene-derived SSR-markers in barley (Hordeum vulgare L.). *Theor Appl Genet* 106(3):411–422.

32. Nielsen H, Engelbrecht J, Brunak S, von Heijne G (1997) Identification of prokaryotic and eukaryotic signal peptides and prediction of their cleavage sites. *Protein Eng* 10(1):1–6.

33. Emanuelsson O, Nielsen H, Brunak S, von Heijne G (2000) Predicting subcellular localization of proteins based on their N-terminal amino acid sequence. *J Mol Biol* 300(4):1005–16.

34. Sonnhammer EL, von Heijne G, Krogh A (1998) A hidden Markov model for predicting transmembrane helices in protein sequences. *Proc Int Conf Intell Syst Mol Biol* 6:175–82.

35. Lahrmann U, et al. (2015) Mutualistic root endophytism is not associated with the reduction of saprotrophic traits and requires a noncompromised plant innate immunity. *New Phytol* 207(3):841–857.

36. Walker JF, et al. (2011) Diverse Helotiales associated with the roots of three species of Arctic Ericaceae provide no evidence for host specificity. *New Phytol* 191(2):515–527.

37. Davies KA, et al. (2000) Evidence for a role of cutinase in pathogenicity of Pyrenopeziza brassicae on brassicas. *Physiol Mol Plant Pathol* 57(2):63–75.

Supplementary tables S1 to S6

Table S1. *Arabis alpina* accessions used in this study.

Accession		**PM**	**E3**	**F1gal**	**S2**
Origin		Arbas del Puerto, Spain	Angliru, Spain	Galibier, France	Nuolja, Sweden
Reference		Wang et al., 2009 (1)	Toräng et al., 2015 (2)	Dombrowski et al., 2017 (3)	Toräng et al., 2015 (2)
Characteristics of the soil of origin[a]					
Soil texture		NA	Sandy-loam	Sandy-loam	Loamy-sand
Humus (%)		NA	3.5	3	4
Clay (%)		NA	16	11	6
Silt (%)		NA	31	11	11
pH		NA	6.8	7.25	6.2
Salinity		NA	31	19.5	46
Available[b] (mg/kg)	Nitrate	NA	59.6	13.5	48.6
	Phosphorus	NA	0.6	1.05	13.5
	Potassium	NA	7.7	5.35	27.1
	Calcium	NA	131.4	141.6	151.9
	Magnesium	NA	5.2	9.75	42.9
Reserve[c] (mg/kg)	Phosphorus	NA	68.1	3.7	85.9
	Potassium	NA	116.5	20.65	137.4
	Calcium	NA	5927	69805	5643
	Magnesium	NA	94.3	644.75	618.2

[a] Analysis conducted by the lbu (Laboratory for Soil Analysis, Thun, Switzerland).

[b] H2O extracted.

[c] Ammonium acetate EDTA extracted (AAE10), representing the plant-available concentrations.

Table S2. Soil characteristics[a].

Soil acronym		Gal	Lau	RecNPK	RecNK
Location		Alps, Col du Galibier	Alps, Col du Lautaret	Agroscope, Reckenhloz	Agroscope, Reckenhloz
Country		France	France	Switzerland	Switzerland
Usage		Natural soil	Botanical garden	Agricultural field	Agricultural field
Sampling time		September 2013	September 2013	May 2013	May 2013
Soil texture		Sandy-loam	Sandy-loam	Sandy-loam	Sandy-loam
Humus (%)		3	3.5	4	4
Clay (%)		11	16	11	11
Silt (%)		11	21	21	21
pH		7.25	7	7.2	7
Salinity		19.5	26	NA	NA
Available[b] (mg/kg)	Nitrate	13.5	42.1	26.1	23.5
	Phosphorus	1.05	11.9	1.6	0.7
	Potassium	5.35	27.6	6.4	4.9
	Calcium	141.6	143.2	182.6	81.2
	Magnesium	9.75	19.7	10.7	14.9
Reserve[c] (mg/kg)	Phosphorus	3.7	106.9	45.4	14.1
	Potassium	20.65	132.3	87.5	101.4
	Calcium	69805	9623	15760	2803
	Magnesium	644.75	306	368.5	284.6
	Br	NA	NA	0.7	0.6
	Mn	NA	NA	382	460
	Cu	NA	NA	15.2	11.5
	Fe	NA	NA	196	177

[a] Analysis conducted by the lbu (Laboratory for Soil Analysis, Thun, Switzerland).

[b] H2O extracted.

[c] Ammonium acetate EDTA extracted (AAE10), representing the plant-available concentrations.

Table S3. Comparison of fungal communities (diversity and structure) across treatments and compartments.

Factor	Groups compared	Differences between the groups: Alpha diversity [a] R^2	Alpha diversity [a] *P*	Community structure [b] R^2	Community structure [b] *P*
Greenhouse experiment (GrH), A. alpina accession PM					
Compartment	BS vs Rhizosphere vs Root	**70%**	**≤ 10^{-4}**	**29%**	**≤ 10^{-4}**
Soil geographical origin	Reckenholz (GrH-RecNK, GrH-RecNPK) vs Lautaret (GrH-Lau)	0%	NS	**21%**	**≤ 10^{-4}**
Soil fertilization regime [c]	GrH-RecNK vs GrH-RecNPK	0%	NS	**6.3%**	**≤ 10^{-4}**
Compartment × Soil geographical origin	(Interaction between the factors)	0%	NS	**10%**	**≤ 10^{-4}**
Compartment × Soil fertilization regime	(Interaction between the factors)	0%	NS	**4%**	**0.01**
Within the root compartment					
Soil geographical origin	Reckenholz (GrH-RecNK, GrH-RecNPK) vs Lautaret (GrH-Lau)	0%	NS	**30%**	**≤ 10^{-4}**
Soil fertilization regime [c]	GrH-RecNK vs GrH-RecNPK	0%	NS	**15%**	**≤ 10^{-4}**
Within the rhizosphere compartment					
Soil geographical origin	Reckenholz (GrH-RecNK, GrH-RecNPK) vs Lautaret (GrH-Lau)	0%	NS	**49%**	**≤ 10^{-4}**
Soil fertilization regime [c]	GrH-RecNK vs GrH-RecNPK	0%	NS	**13%**	**0.004**
Within the bulk soil compartment					
Soil geographical origin	Reckenholz (GrH-RecNK, GrH-RecNPK) vs Lautaret (GrH-Lau)	**82%**	**0.001**	**67%**	**0.001**
Soil fertilization regime [c]	GrH-RecNK vs GrH-RecNPK	0%	NS	**14%**	**0.02**

Greenhouse (GrH) and alpine garden (GAR) experiment, A. alpina accession PM					
Compartment	BS vs Rhizosphere vs Root	**66%**	**≤ 10^{-4}**	**38%**	**≤ 10^{-4}**
Plant growing environment	GAR-Lau vs GrH-Lau	0%	NS	**10%**	**0.002**
Compartment ×Plant growing environment	(Interaction between the factors)	0%	NS	**8%**	**0.04**
Within the root compartment					
Plant growing environment	GAR-Lau vs GrH-Lau	0%	NS	**30%**	**0.003**
Within the rhizosphere compartment					
Plant growing environment	GAR-Lau vs GrH-Lau	0%	NS	**21%**	**0.002**
Within the bulk soil compartment					
Plant growing environment	GAR-Lau vs GrH-Lau	0%	NS	0%	NS
Alpine garden experiment (GAR, all A. alpina accessions[d]) and alpine natural site (WILD, 2013 and 2014)					
Compartment	BS vs Rhizosphere vs Root	**71%**	**≤ 10^{-4}**	**21%**	**≤ 10^{-4}**
Soil	GAR-Lau vs WILD-Gal(2013, 2014)	**9.5%**	**≤ 10^{-4}**	**20%**	**≤ 10^{-4}**
Compartment × Soil	(Interaction between the factors)	0%	NS	10%	**≤ 10^{-4}**
Within the root compartment					
Soil	GAR-Lau vs WILD-Gal(2013, 2014)	**35%**	**≤ 10^{-4}**	**34%**	**≤ 10^{-4}**
Within the rhizosphere compartment					
Soil	GAR-Lau vs WILD-Gal(2013, 2014)	**28%**	**0.0006**	**37%**	**≤ 10^{-4}**
Within the bulk soil compartment					
Soil	GAR-Lau vs WILD-Gal(2013, 2014)	**57%**	**0.004**	**47%**	**0.01**

All experiments (GrH, GAR, WILD)					
Compartment	BS vs Rhizosphere vs Root	**72%**	**≤ 10^{-4}**	**16%**	**≤ 10^{-4}**
Plant growing condition	GrH-RecNK vs GrH-RecNPK vs GrH-Lau vs GAR-Lau vs WILD-Gal.2013 vs WILD-Gal.2014	**9.4%**	**≤ 10^{-4}**	**32%**	**≤ 10^{-4}**
Compartment × Plant growing condition	(Interaction between the factors)	**3%**	**0.02**	**16%**	**≤ 10^{-4}**
Within the root compartment					
Plant growing condition	GrH-RecNK vs GrH-RecNPK vs GrH-Lau vs GAR-Lau vs WILD-Gal.2013 vs WILD-Gal.2014	**50%**	**≤ 10^{-4}**	**49%**	**≤ 10^{-4}**
Within the rhizosphere compartment					
Plant growing condition	GrH-RecNK vs GrH-RecNPK vs GrH-Lau vs GAR-Lau vs WILD-Gal.2013 vs WILD-Gal.2014	**37%**	**0.0006**	**59%**	**≤ 10^{-4}**
Within the bulk soil compartment					
Plant growing condition	GrH-RecNK vs GrH-RecNPK vs GrH-Lau vs GAR-Lau vs WILD-Gal.2013 vs WILD-Gal.2014	**89%**	**≤ 10^{-4}**	**83%**	**≤ 10^{-4}**

[a] Alpha diversity was compared based on one or two factor ANOVA on Shannon's H index ($P < 0.05$)
[b] Community structures were compared based on PerMANOVA on Bray-Curtis dissimilarities ($P < 0.05$, 10.000 permutations).
[c] The soil fertilization regime was studied as a nested factor within soil geographical origin.
[d] As the four *A. alpina* accessions exhibited similar fungal communities in the garden experiment (GAR) (see Fig. S2) combined data from all accession where included in the GAR-Lau treatment, unless indicated otherwise.

Table S4. Primers used.

Tagged primer name	Tag set code[b]	Tagged primer sequence[c]
Forward primers		
ITS9_0	0	catgcgGAACGCAGCRAAIIGYGA
ITS9_1	1	gcagtGAACGCAGCRAAIIGYGA
ITS9_2	2	tagctGAACGCAGCRAAIIGYGA
ITS9_3	3	gactgtGAACGCAGCRAAIIGYGA
ITS9_4	4	cgtcgaGAACGCAGCRAAIIGYGA
ITS9_5	5	gtcgcGAACGCAGCRAAIIGYGA
ITS9_6	6	acgtaGAACGCAGCRAAIIGYGA
ITS9_7	7	cactacGAACGCAGCRAAIIGYGA
ITS9_8	8	tgacGAACGCAGCRAAIIGYGA
ITS9_9	9	agtaGAACGCAGCRAAIIGYGA
ITS9_10	10	atgaGAACGCAGCRAAIIGYGA
ITS9_11	11	tgcaGAACGCAGCRAAIIGYGA
fITS7_0	0	catgcgGTGARTCATCGAATCTTTG
fITS7_1	1	gcagtGTGARTCATCGAATCTTTG
fITS7_2	2	tagctGTGARTCATCGAATCTTTG
fITS7_3	3	gactgtGTGARTCATCGAATCTTTG
fITS7_4	4	cgtcgaGTGARTCATCGAATCTTTG
fITS7_5	5	gtcgcGTGARTCATCGAATCTTTG
fITS7_6	6	acgtaGTGARTCATCGAATCTTTG
fITS7_7	7	cactacGTGARTCATCGAATCTTTG
fITS7_8	8	tgacGTGARTCATCGAATCTTTG
fITS7_9	9	agtaGTGARTCATCGAATCTTTG
fITS7_10	10	atgaGTGARTCATCGAATCTTTG
fITS7_11	11	tgcaGTGARTCATCGAATCTTTG
gITS7_0	0	catgcgGTGARTCATCGARTCTTTG
gITS7_1	1	gcagtGTGARTCATCGARTCTTTG
gITS7_2	2	tagctGTGARTCATCGARTCTTTG
gITS7_3	3	gactgtGTGARTCATCGARTCTTTG
gITS7_4	4	cgtcgaGTGARTCATCGARTCTTTG
gITS7_5	5	gtcgcGTGARTCATCGARTCTTTG
gITS7_6	6	acgtaGTGARTCATCGARTCTTTG
gITS7_7	7	cactacGTGARTCATCGARTCTTTG
gITS7_8	8	tgacGTGARTCATCGARTCTTTG
gITS7_9	9	agtaGTGARTCATCGARTCTTTG
gITS7_10	10	atgaGTGARTCATCGARTCTTTG
gITS7_11	11	tgcaGTGARTCATCGARTCTTTG

Reverse primers

ITS4_0	0	cgcatgTCCTCCGCTTATTGATATGC
ITS4_1	1	actgcTCCTCCGCTTATTGATATGC
ITS4_2	2	agctaTCCTCCGCTTATTGATATGC
ITS4_3	3	acagtcTCCTCCGCTTATTGATATGC
ITS4_4	4	tcgacgTCCTCCGCTTATTGATATGC
ITS4_5	5	gcgacTCCTCCGCTTATTGATATGC
ITS4_6	6	tacgtTCCTCCGCTTATTGATATGC
ITS4_7	7	gtagtgTCCTCCGCTTATTGATATGC
ITS4_8	8	gtcaTCCTCCGCTTATTGATATGC
ITS4_9	9	tactTCCTCCGCTTATTGATATGC
ITS4_10	10	tcatTCCTCCGCTTATTGATATGC
ITS4_11	11	tgcaTCCTCCGCTTATTGATATGC

[a] Primer and tag information are given for the three primer sets used in the primer comparison preliminary study. The same primer/tag combinations were used in the final study with primers ITS9/ITS4.

[b] Tag codes and tag sequences are the same as described by Gloor et al. (2010).

[c] All three forward primers have degenerated positions (R and/or Y) and primer ITS9 has two Inosine residues (I) able to bind to the four nucleotides.

Table S5. Sequence analysis summary.

	Quality-filtered reads[a]		Final reads[b]		Fungal reads[c]		Fungal OTUs[d]	
	Reads ($\times 10^3$)	St. dev.	Reads ($\times 10^3$)	St. dev.	Reads ($\times 10^3$)	St. dev.	OTU	St. dev.
Bulk soil	55.19283	12.15677	52.15817	10.26361	49.36644	10.08392	810.8889	268.0059
Root	55.33284	12.58896	54.48696	12.70806	25.6302	14.51113	232.16	75.72813
Rhizosphere	52.55304	11.72677	50.12016	11.30901	47.23426	10.33892	814.58	198.6037

[a] Number of paired-end reads per sample after sequence quality filtering based on a minimum of 5 bases overlap between the forward and reverse reads (no mismatches), and an absence of mismatches with the primer-tag sequence. This includes fungal and non-fungal reads.

[b] Number of final reads per sample after chimera filtering and removal of low-abundance OTU. This includes fungal and non-fungal reads.

[c] Final number of fungal reads per sample after removing non-fungal reads.

[d] Final number of fungal OTU per sample after removing non-fungal reads.

Table S6. Effect of fungi F229 and F240 on *A. alpina* F1gal growth under gnotobiotic MS agar conditions [a].

Experiment	P level	Treatment	Root				Shoot			
			Length (cm)		Area (cm2)		Weight (mg)		P (µg/mg dw)	
			Mean	S.E.	Mean	S.E.	Mean	S.E.	Mean	S.E.
Effect of F229 on A. alpina F1gal growth [b]										
1	High P	Mock	20.29	1.07	0.41	0.02	29.68	1.61	1332.42	22.90
		F229	22.56	0.95	0.44	0.02	25.28	1.95	1224.15	32.98
	Low P	Mock	19.13	1.67	0.39	0.03	23.76	2.02	277.37	33.39
		F229	**25.03 ****	**1.16**	**0.54 ****	**0.03**	22.54	1.26	217.10	12.09
2	High P	Mock	43.47	2.93	0.84	0.06	46.28	2.76	1447.44	32.98
		F229	42.61	3.23	0.80	0.06	46.76	4.15	1437.35	70.93
	Low P	Mock	33.66	1.37	0.67	0.03	29.58	1.16	235.63	12.21
		F229	33.77	1.35	**0.77 ***	**0.03**	28.95	1.11	228.72	8.53
3	High P	Mock	41.14	2.02	0.78	0.05	47.76	2.43	1643.98	80.67
		F229	42.21	1.85	0.83	0.05	46.15	1.87	1680.09	64.64
	Low P	Mock	28.10	1.41	0.59	0.04	31.15	1.19	487.18	20.32
		F229	**32.65 ***	**1.24**	**0.66 .**	**0.02**	30.87	1.22	558.00	25.06
Effect of F229 and F240 on A. alpina F1gal growth under low P conditions [c]										
4	Low P	Mock	17.45	0.80	0.44	0.03	31.04	1.77		
		F229	**24.25 *****	**1.00**	**0.69 *****	**0.03**	31.41	1.28		
		F240	**29.95 *****	**1.07**	**0.97 *****	**0.06**	33.13	1.26		
5	Low P	Mock	21.46	1.08	0.86	0.06	29.45	1.11		
		F229	**22.77 .**	**1.01**	0.87	0.04	28.72	1.24		
		F240	**24.57 ***	**1.57**	0.83	0.05	29.52	1.18		
6	Low P	Mock	20.33	0.98	0.80	0.04	32.06	1.27		
		F229	**23.88 ***	1.06	0.84	**0.05**	29.08	1.09		
		F240	**26.65 ****	**1.11**	**0.98 ****	**0.05**	31.53	1.09		

[a] Within each experiment statistical differences between Mock and fungus inoculated treatments are indicated in bold (two-sided *t*-test, "." $P < 0.1$, "*" $P < 0.05$, "**" $P < 0.01$) ($n = 14 – 18$ plants per treatment per experiment).

[b] Compiled results from the three experiments shown here are depicted in figure S6 A.

[c] Compiled results from the three experiments shown here are depicted in figure S6 D.

Supplementary figures S1 to S13

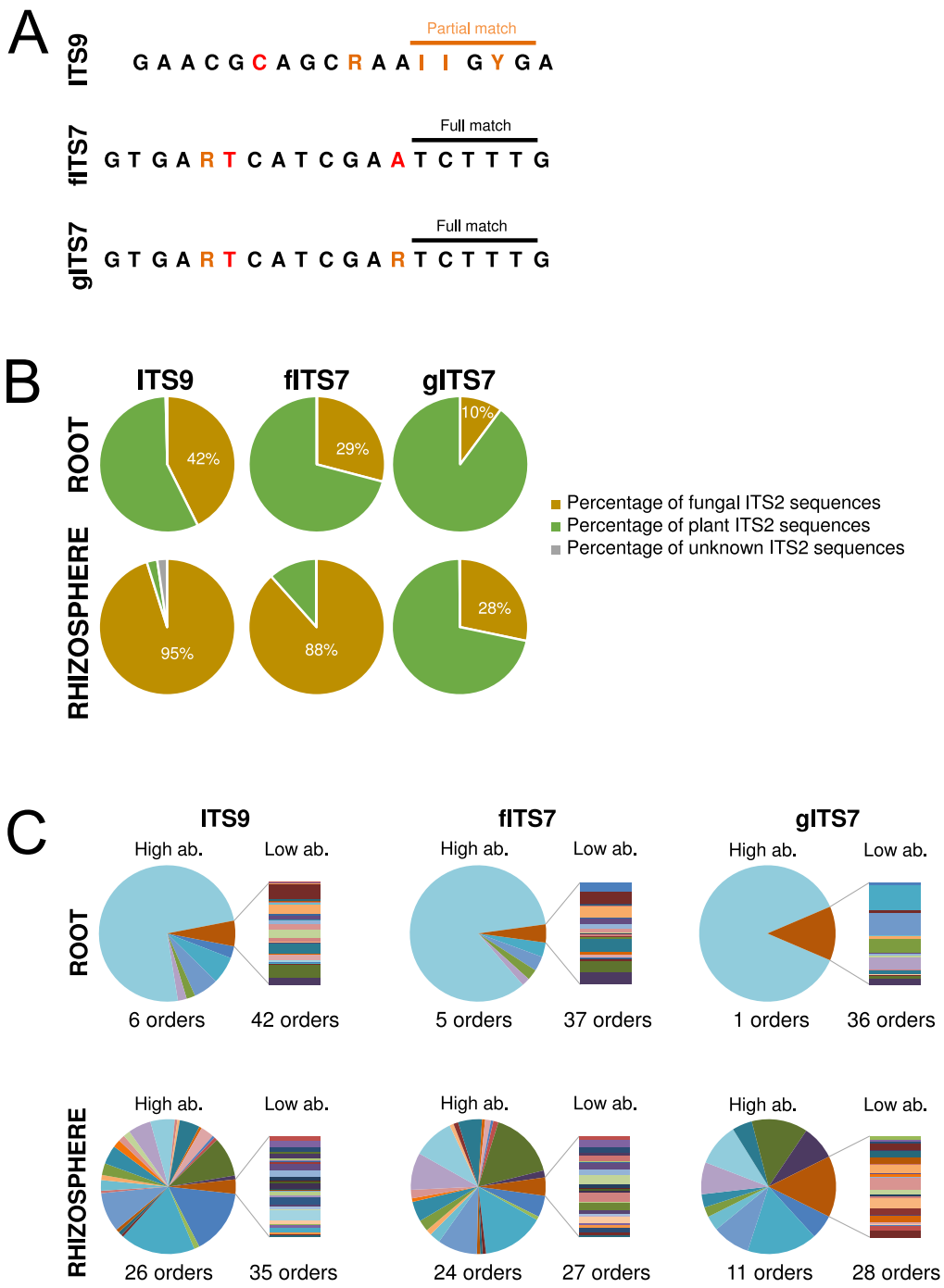

Fig. S1. Comparison of forward primers ITS9, fITS7 and gITS7 in fungal and plant ITS2 amplification. (A) Sequence similarity between the primers and their binding site on *A. alpina* ITS2 region. Fully matching bases are indicated in black, mismatches in red and partially matching bases in orange. All three primers have degenerated positions (R and/or Y) and primer ITS9 has two Inosine residues (I) able to bind to the four nucleotides. (B) Average percentage of unknown, plant and fungal ITS2 sequences amplified with the three primers. Forward primer ITS9 recovered more fungal ITS2 sequences than the other two forward primers (paired t-test, $P < 0.05$). (C) Fungal orders recovered by the three primer pairs. The average relative abundance of each fungal order is shown. The number of high abundance (High ab., > 0.5%) and low abundance (Low ab., <0.5%) fungal orders recovered with each primer is indicated. Forward primer ITS9 recovered more low-abundance fungal orders than the other two forward primers (paired t-test, $P < 0.05$). The three forward primers were tested in combination with reverse primer ITS4 on the same *A. alpina* root (n=3) and rhizosphere (n=3) samples in a preliminary experiment.

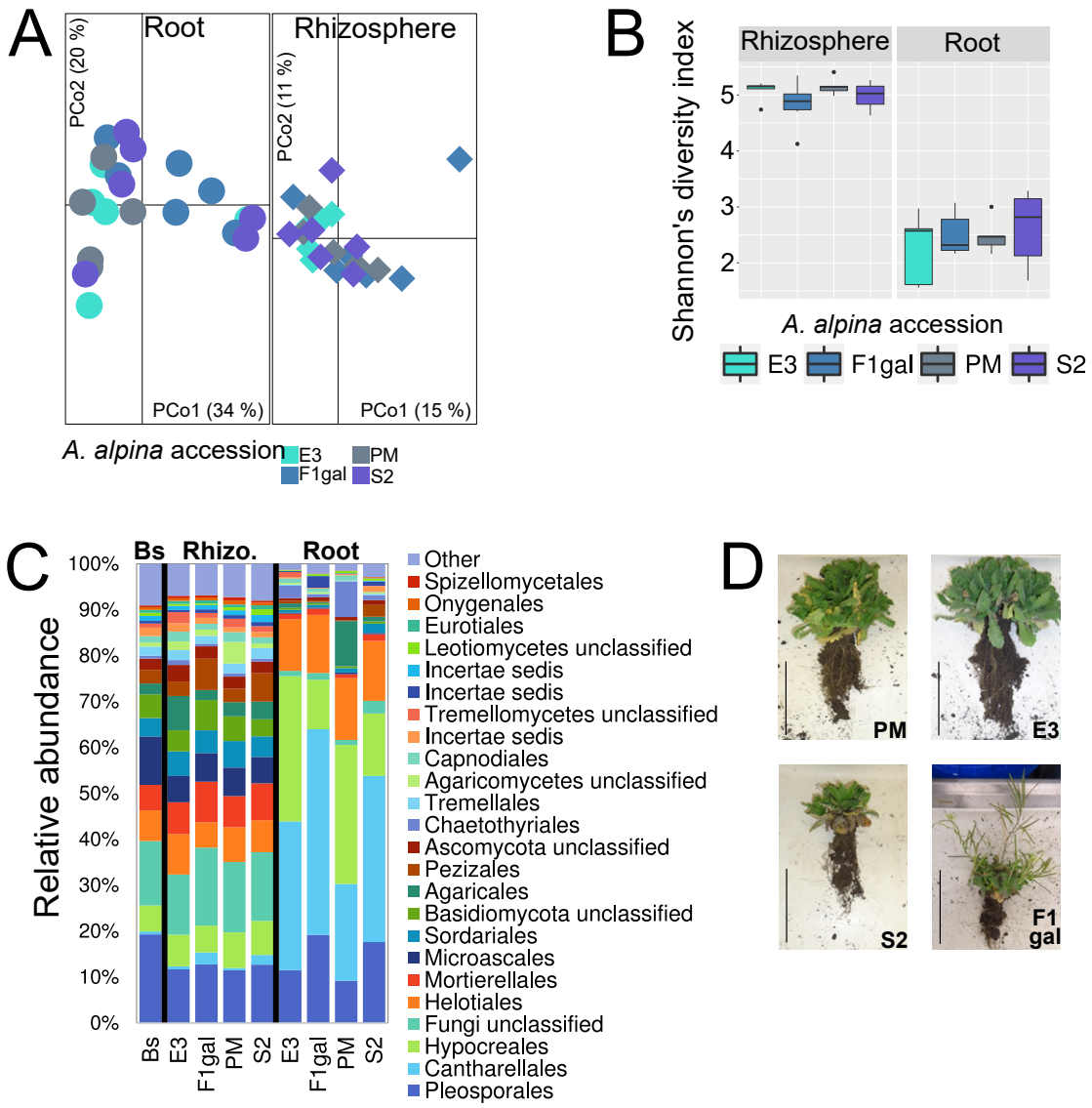

Fig. S2. Comparison of the root and rhizosphere fungal communities colonizing the four *Arabis alpina* accessions in the common garden experiment. (A) Principal coordinate analysis on fungal community differences (Bray-Curtis dissimilarities). (B) Fungal alpha diversity estimated by Shannon's diversity index. (C) Mean relative abundance of the major fungal orders in the different treatments and compartments: bulk soil (Bs), rhizosphere (Rhizo.) and root (Root). (D) *A. alpina* plants at the time of sampling. Accessions PM, E3 and S2 were in a vegetative state while F1gal was at the end of flowering. The scale bar represents 10 cm.

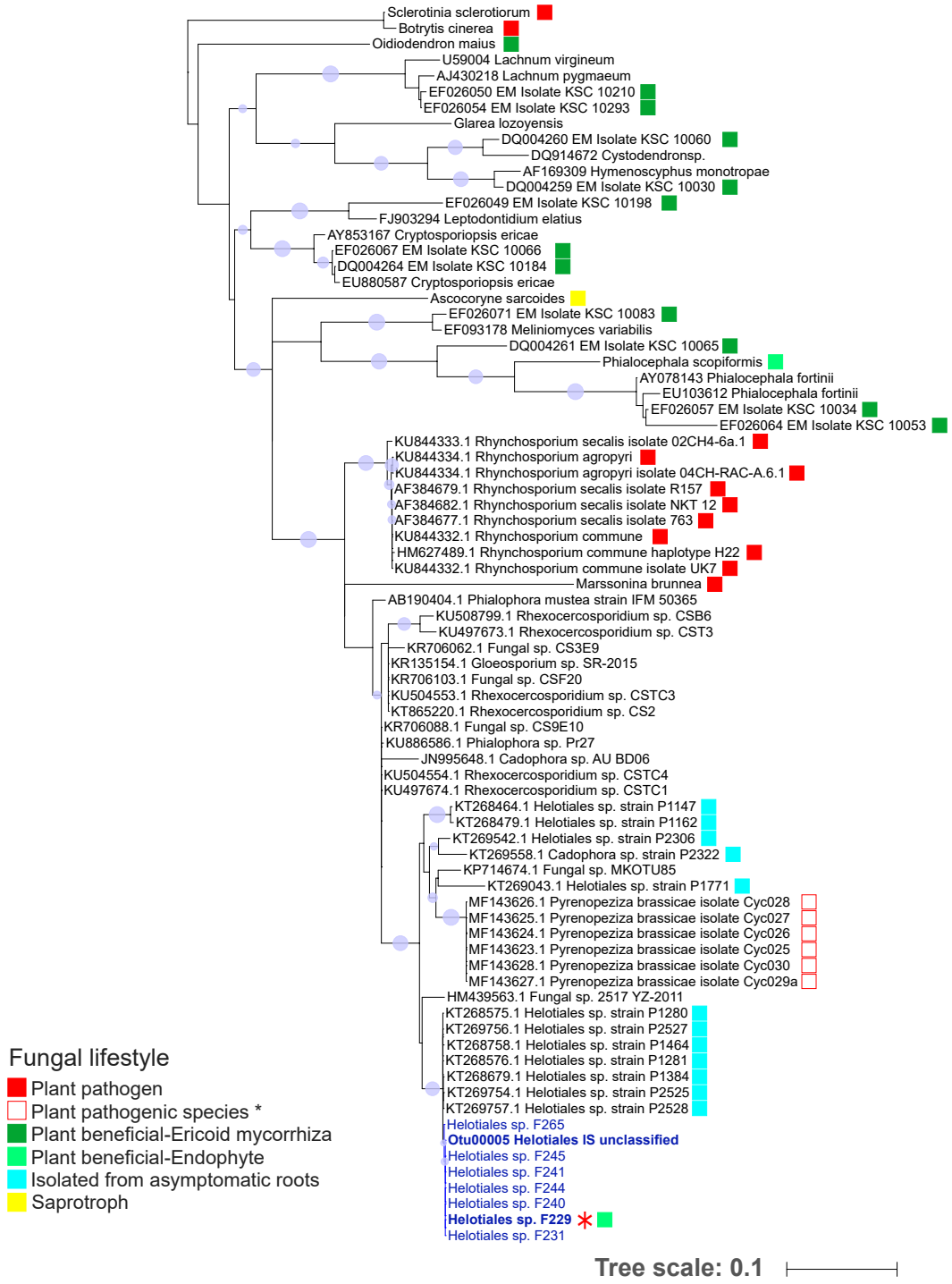

Fig. S3. ITS-based maximum likelihood phylogenetic tree of F229 and the six other isolates belonging to OTU00005 (shown in blue). The analysis includes (i) ITS sequences sharing high similarity with the ITS sequences from F229 and OTU0005 (found by Blast search against the NCBI nr data base, first 20 hits), (ii) sequences from ericoid mycorrhizal Helotiales and their closest relatives (described in Walker *et al.* (2011) (36)) and (iii) sequences from Helotiales with available genome information (shown in Fig. 4). Sequences were aligned with Muscle and the tree was constructed with PhyML (GTR+I+γ model, SH-aLRT method for branch support 1000 iterations under Seaview). Blue dots indicate bootstrap values > 0.8. F229 is shown in bold with a red asterisk. Squares indicate the fungus lifestyle when available. (*) Lifestyle information for the *Pyrenopeziza brassicae* isolates was unavailable but the species is described as plant pathogenic (37).

A

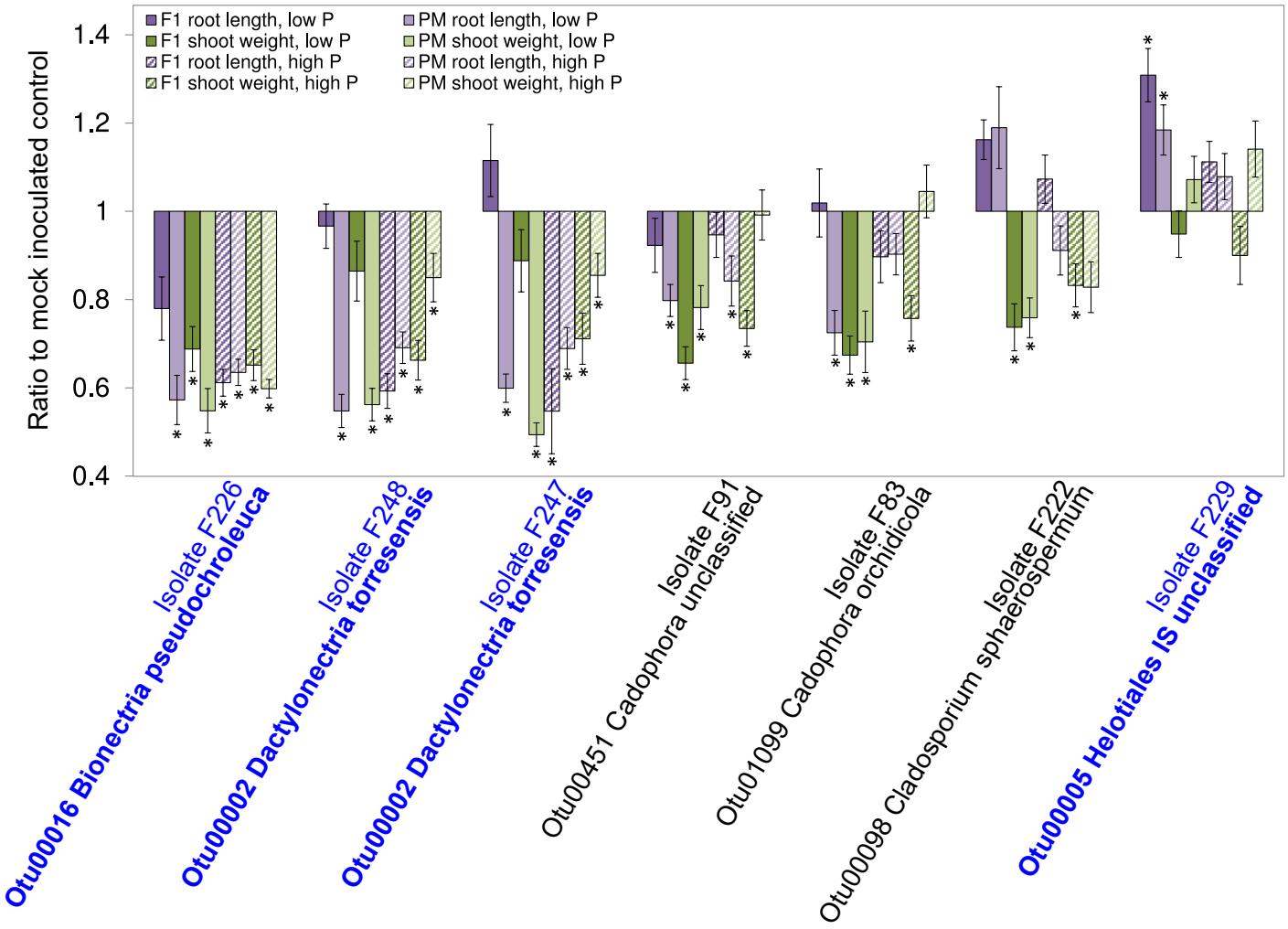

B

Experiment	Plant	P levels	Fungal isolates tested
1	F1	Low and High	F226,F247,F248
2	F1	Low and High	F83,F91,F222,F229
3	PM	Low and High	F222,F226
4	PM	Low and High	F83,F91,F229,F247,F248

Fig. S4. Screening of fungal isolates for their effect on *A. alpina* root and shoot growth on MS agar. (A) Fungal isolates belonging or not to highly-conserved root OTUs (> 85% prevalence in roots, see Fig. 2, shown in blue) were inoculated on *A. alpina* accessions F1gal and PM, under high (1000 µM P) and low (100 µM P) phosphorus conditions. At 14 dpi plant shoot weight and root length were recorded and compared to the mock inoculated controls (n = 16). Ratios to the mock inoculated controls are shown. Means and standard errors are shown. Asterisks indicate a significant difference between mock inoculated and fungus inoculated plants based on t-test (* $P < 0.05$). (B) Experimental set-up. The fungal isolates were screened once in four experiments: two experiments where conducted with each plant accession and each experiment included 2 to 5 fungal isolates. Only results from fungi tested in the same experiment are directly comparable.

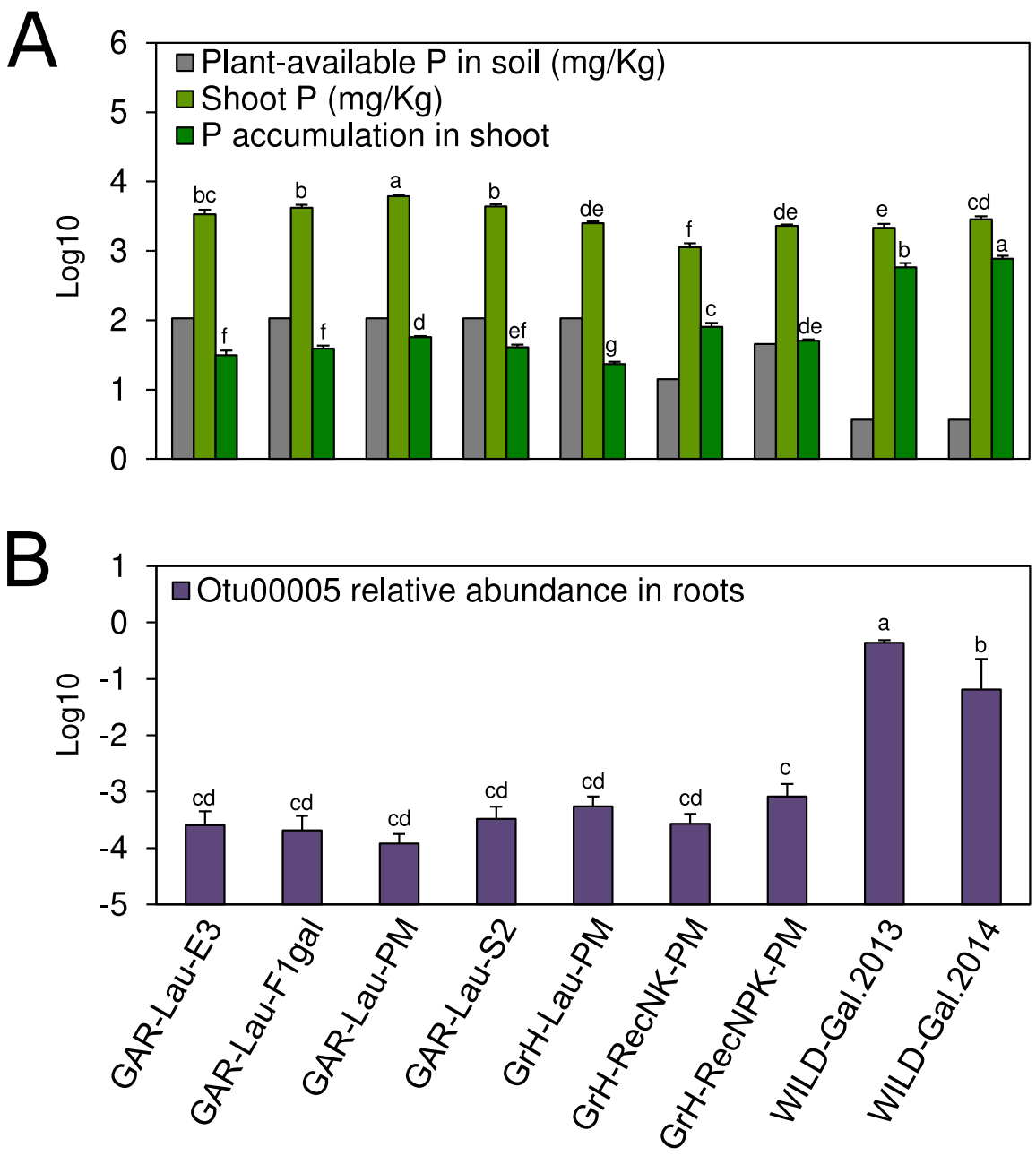

Fig. S5. Relation between P accumulation in the plant shoot and relative abundance of fungal OTU00005 in roots. (A) P concentration in the soil and in the plant shoot, and resulting shoot P accumulation ratio in the different treatments. Plant-available P in the four different soils (see Tab. S2) was measured once using ammonium acetate EDTA extraction (AAE10) by the lbu (Laboratory for Soil Analysis, Thun, Switzerland) (n = 1). Shoot P concentration was measured by ICP-MS on dry shoot material (n = 5 - 6). P accumulation in shoot was calculated for each sample as the ratio between P concentration in the shoot and plant-available P concentration in the soil (n = 5 - 6). (B) Relative abundance of fungal OTU00005 in *A. alpina* roots in the different treatments. Zero values were excluded (n = 43). For each variable, means are shown and error bars represent standard errors, different letters indicate significant differences between the treatments based on ANOVA followed by Tukey's HSD test at $P < 0.05$.

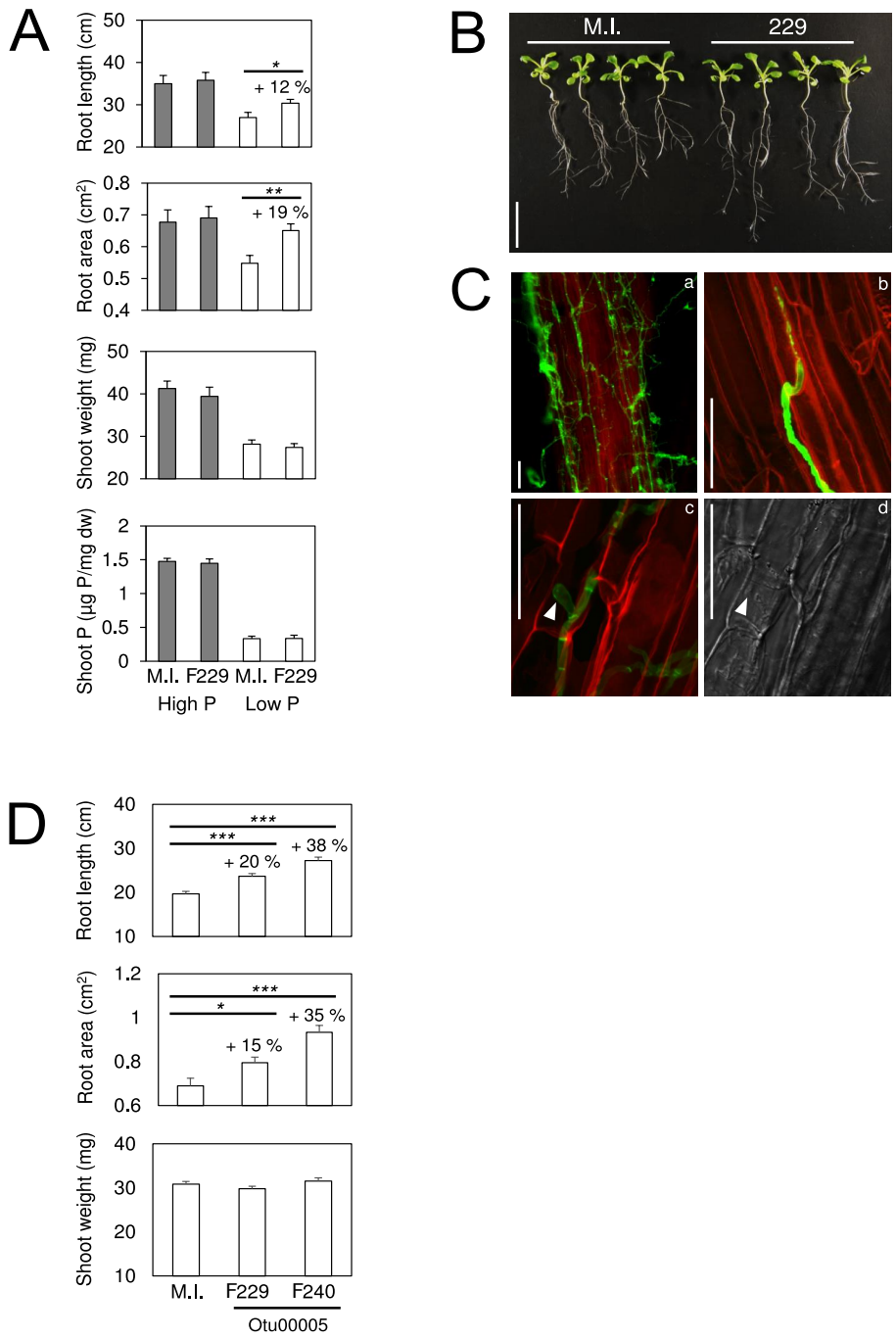

Fig. S6. Root growth promotion and root colonization by F229 (OTU00005) on *A. alpina* F1gal on low P MS agar (14 dpi). (A) Effect of F229 inoculation (F229) on root growth (length and area), shoot weight and shoot P concentration, under high (1000 µM P) and low (100 µM P) phosphorus conditions. Asterisks indicate a significant difference between mock inoculated (M.I.) and inoculated (F229) plants based on *t*-test (* $P < 0.05$, ** $P < 0.01$). The increased percentage is indicated. Compiled results from three experiments are shown (n = 48). Means are shown and error bars represent standard errors. (B) Root-growth promotion upon F229 inoculation under low P conditions. The scale bar represents 2 cm. (C) Root colonization by F229 visualized by confocal microscopy after staining the fungal cell wall with WGA-Alexa (green) and the plant cell wall with propidium iodide (red). The arrows in c and d indicate an intracellular hyphae. The scale bars represents 30 µm. (D) Effect of fungi F229 and F240 (OTU00005) inoculation on shoot weight and root growth (length and area) under low phosphorus conditions. Asterisks indicate a significant difference between mock inoculated (M.I.) and inoculated plants based on *t*-test (* $P < 0.05$, ** $P < 0.01$). The increase percentage is indicated. Compiled results from three experiments are shown (n = 60). Means are shown and error bars represent standard errors. Individual results for each experiment are given in table S6.

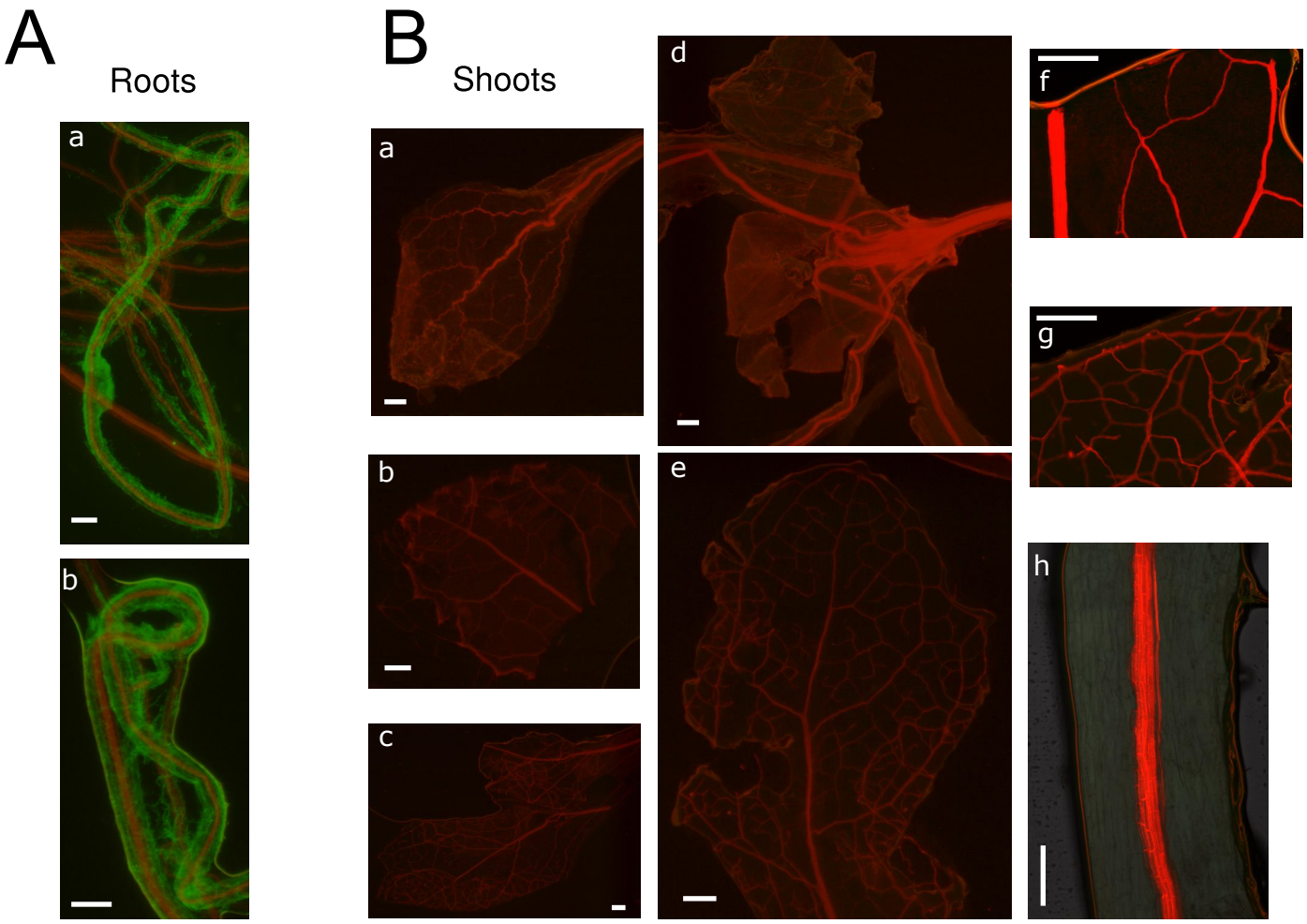

Fig. S7. Absence of fungal colonization of the plant shoot in the ^{33}P transfer experiment. In each ^{33}P transfer experiment (Fig. 3), three fungus inoculated plants were sampled and tested for fungal colonization of the roots and the shoot by fluorescence microscopy after staining the fungal cell wall with WGA-Alexa (green) and the plant cell wall with propidium iodide (red). (A) Representative images showing fungal colonized roots (a-b). (B) Representative images showing fungus free leaves (a-g) and stems (d and h). The scale bars represents 400 µm.

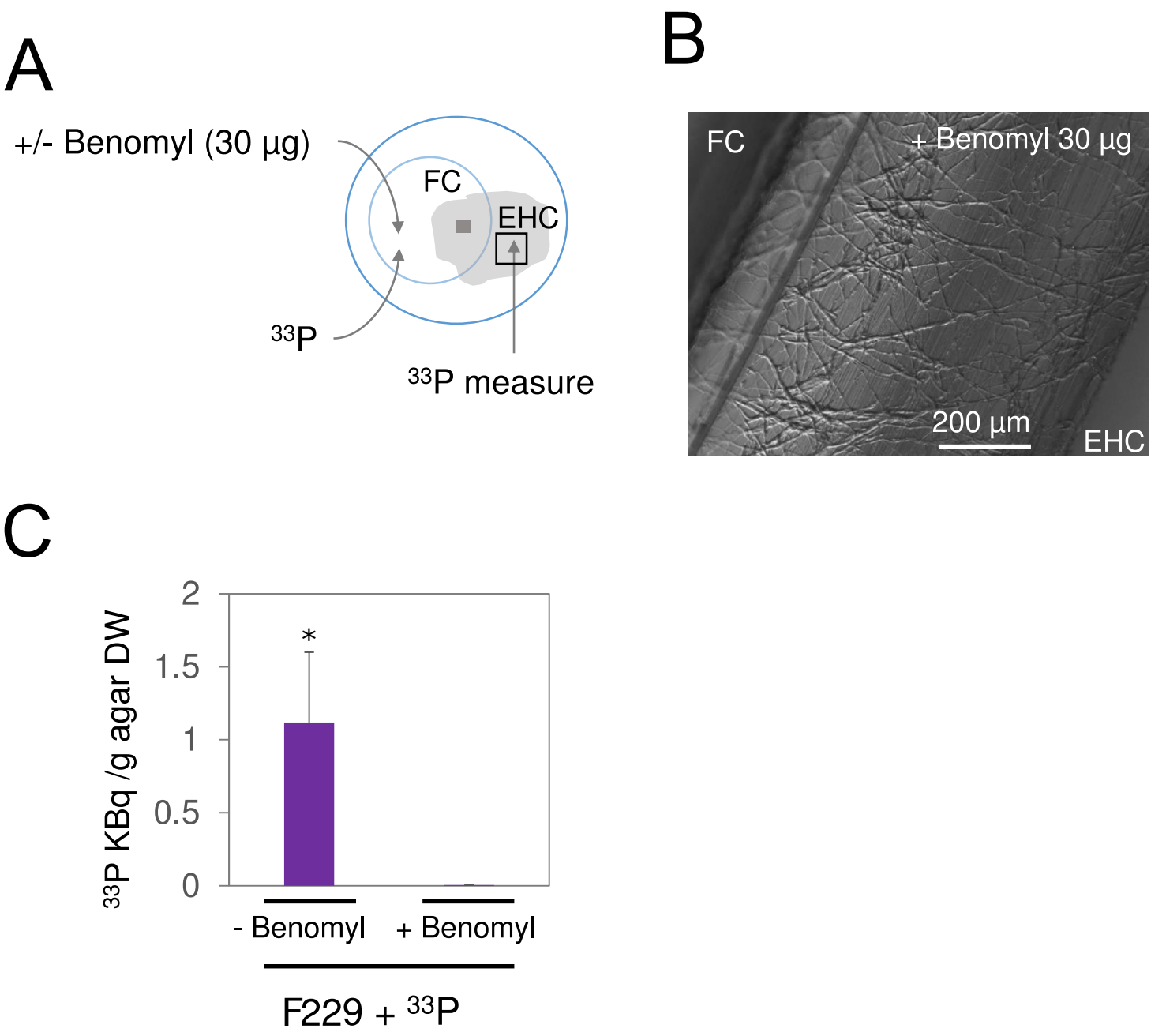

Fig. S8. Effect of Benomyl addition on F229 ^{33}P translocation across compartments. Fungal ^{33}P translocation across the compartments was studied under low P (100 µM P) MS agar in the absence of the plant by sampling an agar piece from the external hyphae compartment (EHC) 7 days after ^{33}P addition in the fungal compartment (FC) previously treated (+ Benomyl) or not (- Benomyl) with Benomyl (30 µg). (A) Experimental set-up. (B) Fungal hyphae crossing the barrier separating the fungal compartment (FC) and the external hyphae compartment (EHC) after Benomyl addition in the FC compartment. (C) ^{33}P measures on the external hyphae compartment (EHC). The asterisk indicates a significant difference between the two treatments based on *t*-test ($P < 0.05$). Compiled results from three experiments are shown (n = 45). Means are shown and error bars represent standard errors.

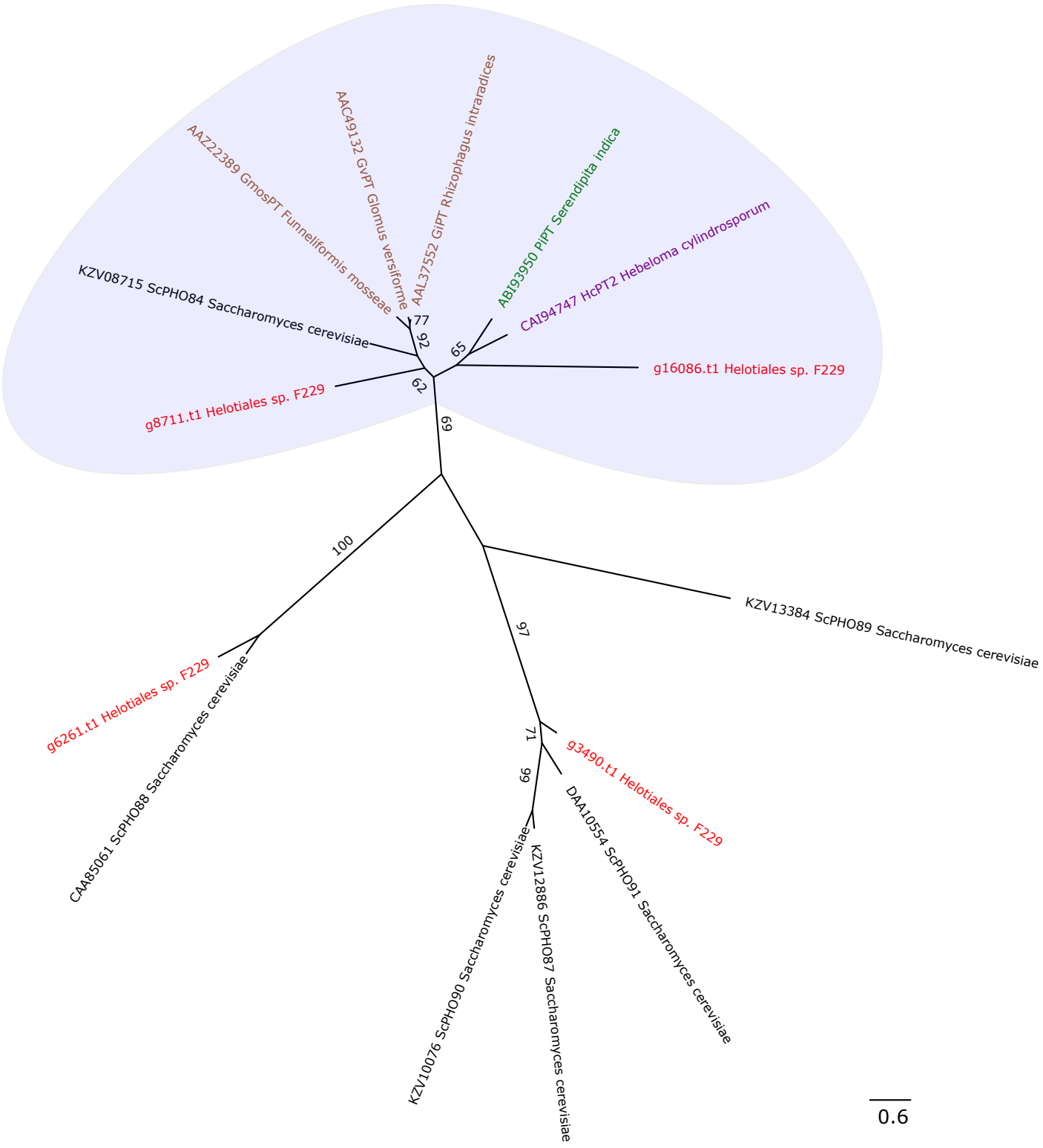

Fig. S9. Unrooted Maximum-Likelihood phylogenetic tree of P transporters in F229 genome. Protein sequences from annotated P transporters (PTs) in F229 genome (shown in red) were compared to described PTs in *Saccharomyces cerevisiae* (ScPHO84, KZV08715 ; ScPHO87, KZV12886 ; ScPHO88 , CAA85061 ; ScPHO89 , KZV13384 ; ScPHO90 , KZV10076 ; ScPHO91; DAA10554) and to fungal PTs known to be involved in fungus to plant P transfer in AM fungi (shown in brown) *Glomus versiforme* (GvPT, Accession number AAC49132), *Rhizophagus intraradices* (GiPT, AAL37552) and *Funneliformis mosseae*, (GmosPT, AAZ22389); the EM fungus (shown in purple) *Hebeloma cylindrosporum* (HcPT2, CAI94747); and the endophytic fungus (shown in green) *Serendipita indica* (PiPT, ABI93950). Protein sequences were aligned using muscle and the phylogenetic reconstruction was conducted using Phy-ML (LG model) under Seaview with 100 bootstrap replicates. Bootstrap values > 60 are shown. PT sequences from F229 genome are given in the Dataset S2. The group of high-affinity PTs is highlighted.

Fig. S10. Maximum likelihood phylogenetic tree of 51 ascomycete genomes, inferred from five housekeeping genes (28S, 18S, Rpb1, Rpb2, EF1alpha). Bootstrap values > 0.8 are shown. *Laccaria bicolor* sequences were used for tree rooting. Helotiales with plant beneficial, plant pathogenic or saprophytic lifestyles are indicated (see legend Fig. 4).

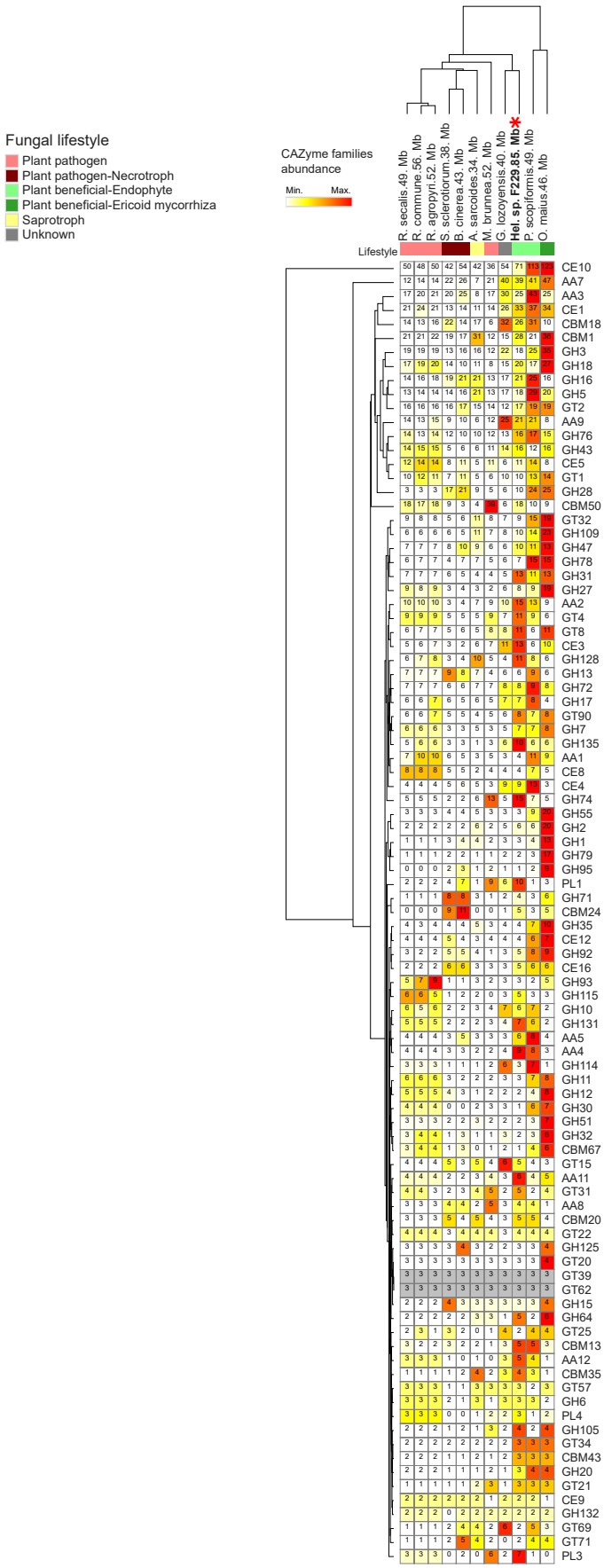

Fig. S11. Hierarchical clustering on the abundance of CAZyme families in F229 and related Helotiales with plant-symbiotic, plant-pathogenic or saprophytic lifestyles. Only high-abundance families (> 20 occurrences in total) are shown. The color scale depicts standardized values for each module. Fungal orders and genome sizes are indicated before and after their name, respectively. Xyl., Xylonales; Xyr., Xylariales; Sor., Sordariales; Pez., Pezizales; Oph., Ophiostomatales; Mag., Magnaporthales; inc., Incertae sedis; Glo., Glomerellales; Hyp., Hypocreales; Hel., Helotiales; Ery., Erysiphales; Dia., Diaporthales; Cap., Capnodiales. F229 is shown in bold with an asterisk. The data is given in the Dataset S3.

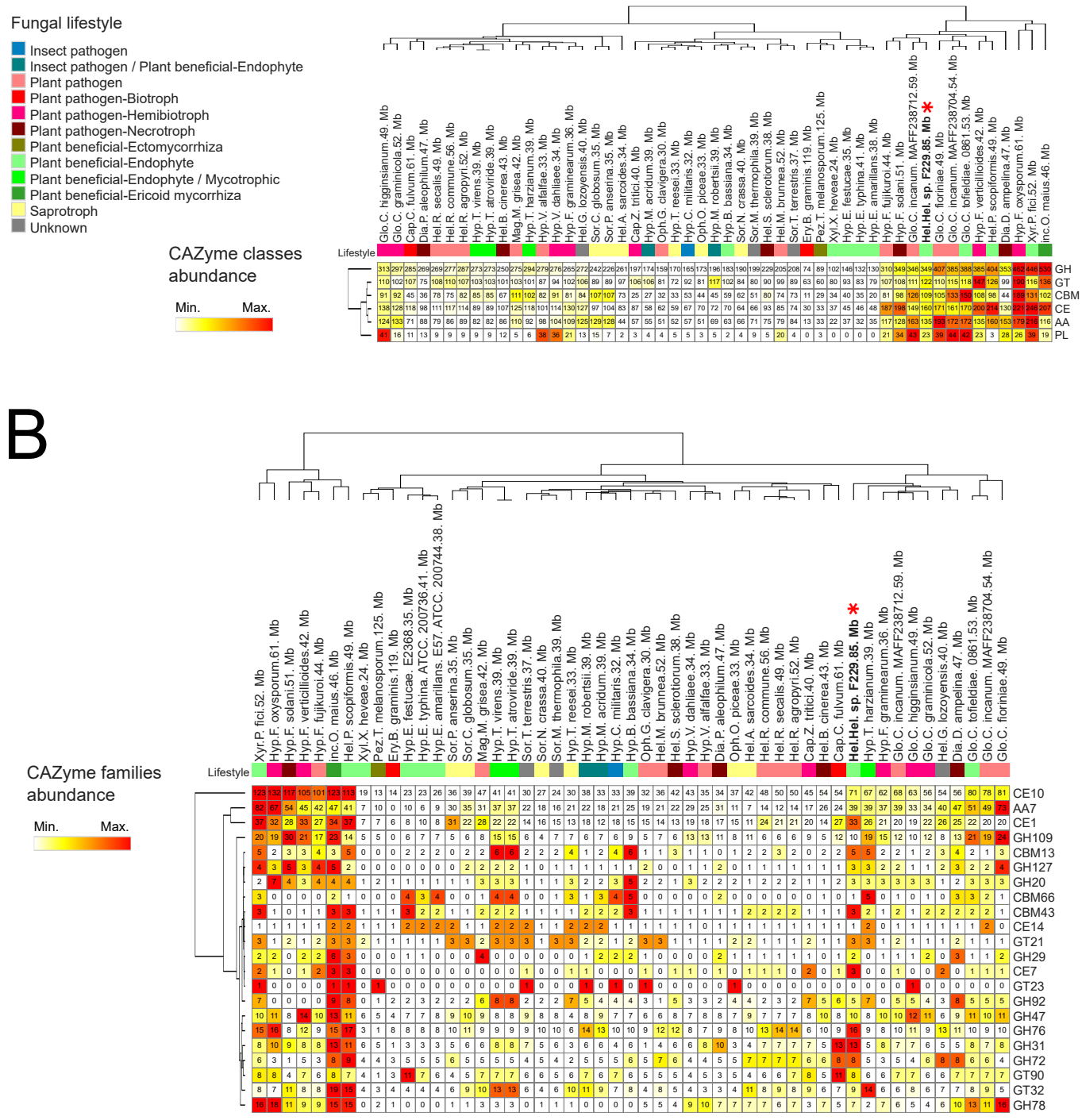

Fig. S12. Hierarchical clustering on the abundance of CAZyme classes and selected families within ascomycetes with plant-symbiotic, plant-pathogenic or saprophytic lifestyles. (A) Abundance of CAZyme classes. (B) Abundance of CAZyme families previously shown to be associated to a plant-symbiotic lifestyle in the Helotiales. In A and B, the color scale depicts maximum and minimum values for each module. Fungal orders and genome sizes are indicated before and after their name respectively. Xyl., Xylonales; Xyr., Xylariales; Sor., Sordariales; Pez., Pezizales; Oph., Ophiostomatales; Mag., Magnaporthales; inc., Incertae sedis; Glo., Glomerellales; Hyp., Hypocreales; Hel., Helotiales; Ery., Erysiphales; Dia., Diaporthales; Cap., Capnodiales. F229 is shown in bold with an asterisk. The data is given in the Dataset S3.

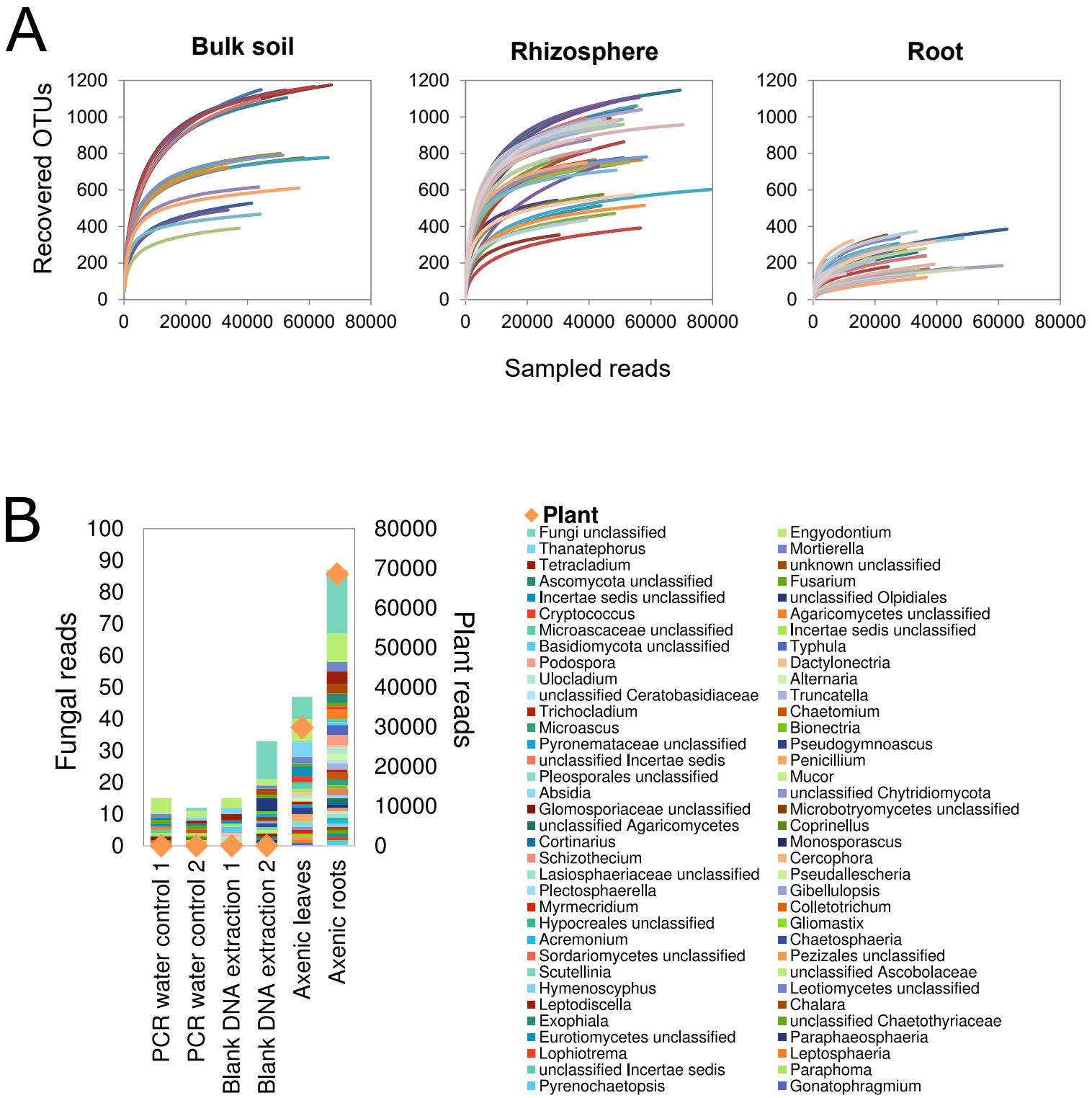

Fig. S13. Rarefaction curves and negative control samples. (A) Rarefaction curves inferred from bulk soil, root and rhizosphere ITS2 fungal reads. The number of new OTUs recovered was assessed after re-sampling 100 reads without replacement for 1000 iterations in Mothur. (B) Environmental and seed-derived contamination during fungal ITS2 sequencing. Number of plant (Orange diamonds) and fungal (bars) reads detected in the different control samples. Less than 40 reads were obtained in the negative controls ('PCR water control' and 'Blank DNA extraction') indicating low environmental and kit-derived fungal contamination. Less than 90 fungal genera were detected in leaves and shoots of axenic ally grown plants ('Axenic leaves' and 'Axenic roots') indicating low seed-derived fungal contamination.